Relativistic many-body calculations of excitation energies, oscillator strengths, transition rates, and lifetimes in samariumlike ions

U. I. Safronova and A. S. Safronova
Physics Department, University of Nevada, Reno, Nevada 89557, USA

P. Beiersdorfer
Physics Division, Lawrence Livermore National Laboratory, Livermore, California 94550, USA

(Received 21 January 2013; published 12 March 2013)

The unique atomic properties of samariumlike ions, not yet measured experimentally, are theoretically predicted and studied in this paper. Excitation energies, oscillator strengths, transition probabilities, and lifetimes are calculated for $(5s^2 + 5p^2 + 5d^2 + 5s5d + 5s5g + 5p5f)$–$(5s5p + 5s5f + 5p5d + 5p5g)$ electric dipole transitions in Sm-like ions with nuclear charge Z ranging from 74 to 100. Relativistic many-body perturbation theory (RMBPT), including the Breit interaction, is used to evaluate retarded $E1$ matrix elements in length and velocity forms. The calculations start from a $1s^22s^22p^63s^23p^63d^{10}4s^24p^64d^{10}4f^{14}$ Dirac-Fock potential. First-order perturbation theory is used to obtain intermediate coupling coefficients, and the second-order RMBPT is used to determine the matrix elements. The contributions from negative-energy states are included in the second-order $E1$ matrix elements to achieve agreement between length-form and velocity-form amplitudes. The resulting transition energies and transition probabilities, and lifetimes for Sm-like W^{12+} are compared with results obtained by the relativistic Hartree-Fock approximation (COWAN code) to estimate contributions of the $4f$-core-excited states. Trends of excitation energies and oscillator strengths as the function of nuclear charge Z are shown graphically for selected states and transitions. This work provides a number of yet unmeasured atomic properties of these samariumlike ions for various applications and as a benchmark for testing theory.

DOI: 10.1103/PhysRevA.87.032508 PACS number(s): 31.15.ag, 31.15.am, 31.15.vj, 31.15.aj

I. INTRODUCTION

One of the unique atomic properties of the samarium isoelectronic sequence is that the ground state changes nine times starting from the $[Kr]4d^{10}5s^25p^64f^66s^2\,{}^1S_0$ level for neutral samarium, Sm I, and ending with the $[Kr]4d^{10}4f^{14}5s^2\,{}^1S_0$ level for 12 times ionized tungsten, W^{12+} [1]. The largest number of levels (501) displayed in the NIST database [1] is for Sm I. The number of levels with recommended NIST energies for one time ionized europium, Eu^+ with a $[Kr]4d^{10}5s^25p^64f^76s\,{}^9S_4$ ground level is in three times smaller (163). Only 28 levels are given in the NIST database [1] for two times ionized gadolinium, Gd^{2+}, with a $[Kr]4d^{10}5s^25p^64f^75d\,{}^9D_2$ ground level and the three times ionized terbium, Tb^{3+} with the $[Kr]4d^{10}5s^25p^64f^8\,{}^7F_6$ ground level. A detailed study of the transition probabilities in Gd^{2+} was recently presented by Biémont *et al.* in [2]. Only the ground-state configurations are included in the NIST compilation for other ions of Sm isoelectronic sequence.

In Fig. 1, we plot the one-electron energies of the $4f_j$, $5p_j$, and $5s_{1/2}$ orbitals calculated in Dirac-Fock (DF) approximation as a function of nuclear charge Z. For better presentation, we scaled those energies by a factor of $(Z - 55)^2$. We find that the curve describing the energies of the $5s_{1/2}$ orbital crosses the curves describing the energies of the $4f_{5/2}$ and $4f_{7/2}$ orbitals around $Z = 72$–73. The difference between energies of the $5s_{1/2}$ and $4f_{5/2}$ orbitals for $Z = 72$ is equal to -46 in units $(Z - 55)^2$ cm^{-1}, while the difference between energies of the $5s_{1/2}$ and $4f_{7/2}$ orbitals for $Z = 73$ is equal to 66 in units of $(Z - 55)^2$ cm^{-1}. That leads us to conclude that the $4f_{5/2}$ and $4f_{7/2}$ orbitals are more tightly bound than the $5s_{1/2}$ and $5p_j$ orbitals for larger stages of ionization and that the ground state of Sm-like ions with $\geqslant 74$ will be the $[Kr]4d^{10}4f^{14}5s^2\,{}^1S_0$ level. This conclusion agrees with the NIST database [1] for the Sm-like W^{12+} ion with $Z = 74$, however, the $[Kr]4d^{10}4f^{13}5p$ configuration was found to be the ground state of the Sm-like ions with $Z > 74$. This is very strange because the difference between the energies of the $4f_j$ and $5l_j$ energies increases with Z, as illustrated by Fig. 1, so that the ground state of Sm-like ions with $Z > 74$ should be the same as the ground state of the Sm-like W^{12+} ion with $Z = 74$.

In this paper we report the results of *ab initio* calculations of excitation energies, oscillator strengths, transition probabilities, and lifetimes in Sm-like ions with nuclear charge Z ranging from 74 to 100. We consider these ions as systems with closed $4f^{14}$ core and two electrons above the core as $[Kr]4d^{10}4f^{14}5l5l'$ states. We use the relativistic many-body perturbation theory (RMBPT) to determine the energies of the 34 even-parity $(5s^2 + 5p^2 + 5d^2 + 5s5d + 5p5f)$ states and the 32 odd-parity states for samariumlike ions with nuclear charges in the range $Z = 74$–100. We illustrate our calculations with detailed studies of Sm-like tungsten, $Z = 74$. Our calculations are carried out to second order in perturbation theory and include the second-order Coulomb interaction. Corrections for the frequency-dependent Breit interaction are taken into account in the lowest order. The relativistic MBPT is used to determine reduced matrix elements, oscillator strengths, and transition rates for all allowed and forbidden electric dipole $(5s^2 + 5p^2 + 5d^2 + 5s5d + 5p5f) \Leftrightarrow (5s5p + 5s5f + 5p5d + 5p5g)$ transitions in Sm-like ions. Retarded $E1$ matrix elements are evaluated in both length and velocity forms. The RMBPT calculations starting from a local potential are gauge independent order by order, providing "derivative terms" are included in the second- and higher-order matrix elements and thus careful attention is paid

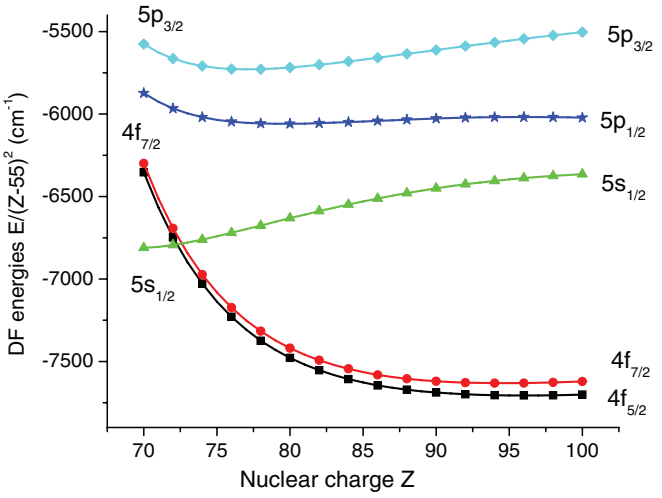

FIG. 1. (Color online) One-electron Dirac-Fock (DF) energies of the $4f_j$, $5s_{1/2}$, and $5p_j$ orbitals as a function of Z for Sm-like ions.

to negative-energy states. The present RMBPT calculations start from a nonlocal $1s^22s^22p^63s^23p^63d^{10}4s^24p^64d^{10}4f^{14}$ Dirac-Fock potential and consequently give gauge-dependent transition matrix elements. Second-order correlation corrections compensate almost exactly for the gauge dependence of the first-order matrix elements, leading to corrected matrix elements that differ by less than 1% in length and velocity forms throughout the periodic system.

Our work is motivated in part by renewed interest in the spectral emission of tungsten from magnetically confined high-temperature plasmas as illustrated by recent publications [3–16]. Tungsten will likely be a constituent of plasmas generated by the ITER (Latin, "the way") tokamak [17], and spectroscopic diagnostics are currently being developed that use radiation from tungsten ions for determining ITER plasma parameters [10,13,18]. An overview of recent results from the Livermore WOLFRAM spectroscopy project was presented recently by Clementson *et al.* [3], which includes experimental investigations at the EBIT-I and SuperEBIT electron beam ion traps. In particular, the spectra of highly charged M- and L-shell tungsten ions were studied [3]. Beiersdorfer *et al.* [4] presented high-resolution crystal spectroscopy measurements of the $n = 3 \rightarrow n = 2L$-shell x-ray transitions of neonlike W^{64+}, which include seven electric-dipole-allowed transitions, two electric quadrupole transitions, and one magnetic quadrupole transition. The possibility of using extreme ultraviolet emission from low-charge states of tungsten ions to diagnose the divertor plasmas of the ITER tokamak was investigated by Clementson *et al.* [7]. Spectral modeling of Lu-like W^{3+} to Gd-like W^{10+} were performed by using the flexible atomic code (FAC), and spectroscopic measurements were conducted at the Sustained Spheromak Physics Experiment (SSPX) in Livermore [7]. Moreover, measurements of spectral emission from tungsten in the extreme ultraviolet were presented by Harte *et al.* [11], who performed their measurements on the Large Helical Device, by Clementson *et al.* [14], who conducted experiments on the National Spherical Torus Experiment, and by Reinke *et al.* [15], who studied plasmas produced by the Alcator tokamak. In parallel, there has been a corresponding theoretical effort to generate atomic data relevant to magnetic fusion plasmas. Dielectronic satellite spectra of Yb-like tungsten (W^{4+}) and Tm-like tungsten (W^{5+}) were presented in [19,20]. Wavelengths, transition rates, and line strengths were calculated recently for the $4f^{13}5p^6nl$- $4f^{14}5p^6$ multipole transitions in Er-like W^{6+} ion [21]. The relativistic many-body perturbation theory, including the Breit interaction, was used to evaluate energies and transition rates for multipole transitions in this hole-particle system. The RMBPT approximation was used in Ref. [22] to study correlation and relativistic effects in the trivalent Lu-like W^{3+} ion. Recently, configuration interaction and radiative decay rates in triply ionized tungsten (W IV) was investigated in Ref. [23]. Numerical results for the first excited configurations ($5d^26s$, $5d6s^2$, $5d^26p$, and $5d6s6p$) were obtained with two independent [i.e., multiconfiguration Dirac-Fock and relativistic Hartree-Fock with core-polarization effects (HFR + CPOL)] methods.

II. METHOD

The RMBPT formalism developed previously [24–34] for Be-, Mg-, Ca-, Zn-, and Yb-like ions is used here to describe the perturbed wave functions, to obtain the second-order energies [24], and to evaluate the first- and second-order transition matrix elements [26,32] in Sm-like ions. The calculations are carried out using a basis set of DF orbitals. The orbitals used in the present calculations are obtained as linear combinations of B splines. These B-spline basis orbitals are determined using the method described in Ref. [35]. We use 50 B splines of order 10 for each single-particle angular momentum state, and we include all orbitals with orbital angular momentum $l \leqslant 9$ in our basis set.

The model space for the $(5s^2 + 5p^2 + 5d^2 + 5s5d + 5p5f)$ and $(5s5p + 5s5f + 5p5d + 5p5g)$ complexes in Sm-like ions has 35 even-parity states and 32 odd-parity states. The 35 even-parity states consist of five $J = 0$ states, four $J = 1$ states, ten $J = 2$ states, seven $J = 3$ states, seven $J = 4$ states, and two $J = 5$ states. Additionally, there are 32 odd-parity states consisting of two $J = 0$ states, five $J = 1$ states, seven $J = 2$ states, eight $J = 3$ states, six $J = 4$ states, three $J = 5$ states, and one $J = 6$ state. The distribution of the 67 states in the model space is summarized in Table I where both jj and LS designations are given. When starting calculations from relativistic Dirac-Fock wave functions, it is natural to use jj designations for uncoupled transition and energy matrix elements; however, neither jj nor LS coupling describes the *physical* states properly, except for the single-configuration state $5d_{5/2}5f_{7/2}(6) \equiv 5d5f\,^3H_6$.

III. EXCITATION ENERGIES IN Sm-LIKE IONS

In Table II, we illustrate the relative size of various contributions before diagonalization using the example of the even-parity states $5l_{j_1}5l'_{j_2}$ with $J = 0$ in Sm-like W^{12+}. The zeroth, first-, and second-order Coulomb contributions $E^{(0)}$, $E^{(1)}$, and $E^{(2)}$, and the first- and second-order Breit-Coulomb corrections $B^{(1)}$ and $B^{(2)}$, are given.

The importance of correlation contributions is evident from this table; the ratio of the first and zeroth orders ($E^{(1)}/E^{(0)}$) is

TABLE I. Two-particle even-parity and odd-parity states in the Sm-like ion.

Even-parity states		Even-parity states		Odd-parity states		Odd-parity states	
jj coupling	LS coupling	jj coupling	LS coupling	jj coupling	LS coupling	jj coupling	LS coupling
$5s_{1/2}5s_{1/2}(0)$	$5s^2\,{}^1S_0$	$5s_{1/2}5d_{5/2}(3)$	$5s5d\,{}^3D_3$	$5s_{1/2}5p_{1/2}(0)$	$5s5p\,{}^3P_0$	$5p_{1/2}5d_{5/2}(3)$	$5p5d\,{}^3D_3$
$5p_{1/2}5p_{1/2}(0)$	$5p^2\,{}^3P_0$	$5p_{1/2}5f_{5/2}(3)$	$5p5f\,{}^1F_3$	$5p_{3/2}5d_{3/2}(0)$	$5p5d\,{}^3P_0$	$5p_{3/2}5d_{3/2}(3)$	$5p5d\,{}^3F_3$
$5p_{3/2}5p_{3/2}(0)$	$5p^2\,{}^1S_0$	$5p_{1/2}5f_{7/2}(3)$	$5p5f\,{}^3F_3$			$5p_{3/2}5d_{5/2}(3)$	$5p5d\,{}^1F_3$
$5d_{3/2}5d_{3/2}(0)$	$5d^2\,{}^3P_0$	$5s_{1/2}5g_{7/2}(3)$	$5s5g\,{}^3G_3$	$5s_{1/2}5p_{1/2}(1)$	$5s5p\,{}^3P_1$	$5s_{1/2}5f_{5/2}(3)$	$5s5f\,{}^3F_3$
$5d_{5/2}5d_{5/2}(0)$	$5d^2\,{}^1S_0$	$5d_{3/2}5d_{5/2}(3)$	$5d^2\,{}^3F_3$	$5s_{1/2}5p_{3/2}(1)$	$5s5p\,{}^1P_1$	$5s_{1/2}5f_{7/2}(3)$	$5s5f\,{}^1F_3$
		$5p_{3/2}5f_{7/2}(3)$	$5p5f\,{}^3G_3$	$5p_{1/2}5d_{3/2}(1)$	$5p5d\,{}^3D_1$	$5p_{1/2}5g_{7/2}(3)$	$5p5g\,{}^3F_3$
$5p_{1/2}5p_{3/2}(1)$	$5p^2\,{}^3P_1$	$5p_{3/2}5f_{5/2}(3)$	$5p5f\,{}^3D_3$	$5p_{3/2}5d_{3/2}(1)$	$5p5d\,{}^3P_1$	$5p_{3/2}5g_{7/2}(3)$	$5p5g\,{}^3G_3$
$5s_{1/2}5d_{3/2}(1)$	$5s5d\,{}^3D_1$			$5p_{3/2}5d_{5/2}(1)$	$5p5d\,{}^1P_1$	$5p_{3/2}5g_{9/2}(3)$	$5p5g\,{}^1F_3$
$5d_{3/2}5d_{5/2}(1)$	$5d^2\,{}^3P_1$	$5p_{1/2}5f_{7/2}(4)$	$5p5f\,{}^3F_4$				
$5p_{3/2}5f_{5/2}(1)$	$5p5f\,{}^3D_1$	$5s_{1/2}5g_{7/2}(4)$	$5s5g\,{}^1G_4$	$5s_{1/2}5p_{3/2}(2)$	$5s5p\,{}^3P_2$	$5p_{3/2}5d_{5/2}(4)$	$5p5d\,{}^3F_4$
		$5s_{1/2}5g_{9/2}(4)$	$5s5g\,{}^3G_4$	$5p_{1/2}5d_{3/2}(2)$	$5p5d\,{}^1D_2$	$5s_{1/2}5f_{7/2}(4)$	$5s5f\,{}^3F_4$
$5p_{1/2}5p_{3/2}(2)$	$5p^2\,{}^3P_2$	$5d_{3/2}5d_{5/2}(4)$	$5d^2\,{}^1G_4$	$5p_{1/2}5d_{5/2}(2)$	$5p5d\,{}^3D_2$	$5p_{1/2}5g_{7/2}(4)$	$5p5g\,{}^3G_4$
$5p_{3/2}5p_{3/2}(2)$	$5p^2\,{}^1D_2$	$5d_{5/2}5d_{5/2}(4)$	$5d^2\,{}^3F_4$	$5p_{3/2}5d_{3/2}(2)$	$5p5d\,{}^3F_2$	$5p_{1/2}5g_{9/2}(4)$	$5p5g\,{}^1G_4$
$5s_{1/2}5d_{3/2}(2)$	$5s5d\,{}^3D_2$	$5p_{3/2}5f_{5/2}(4)$	$5p5f\,{}^3G_4$	$5p_{3/2}5d_{5/2}(2)$	$5p5d\,{}^3P_2$	$5p_{3/2}5g_{7/2}(4)$	$5p5g\,{}^3F_4$
$5s_{1/2}5d_{5/2}(2)$	$5s5d\,{}^1D_2$	$5p_{3/2}5f_{7/2}(4)$	$5p5f\,{}^1G_4$	$5s_{1/2}5f_{5/2}(2)$	$5s5f\,{}^3F_2$	$5p_{3/2}5g_{9/2}(4)$	$5p5g\,{}^3H_4$
$5p_{1/2}5f_{5/2}(2)$	$5p5f\,{}^3F_2$	$5s_{1/2}5g_{9/2}(5)$	$5s5g\,{}^3G_5$	$5p_{3/2}5g_{7/2}(2)$	$5p5g\,{}^3F_2$	$5p_{1/2}5g_{9/2}(5)$	$5p5g\,{}^3G_5$
$5d_{5/2}5d_{5/2}(2)$	$5d^2\,{}^3F_2$	$5p_{3/2}5f_{7/2}(5)$	$5p5f\,{}^3G_5$			$5p_{3/2}5g_{7/2}(5)$	$5p5g\,{}^3H_5$
$5d_{3/2}5d_{5/2}(2)$	$5d^2\,{}^3P_2$					$5p_{3/2}5g_{9/2}(5)$	$5p5g\,{}^1H_5$
$5d_{3/2}5d_{3/2}(2)$	$5d^2\,{}^1D_2$					$5p_{3/2}5g_{9/2}(6)$	$5p5g\,{}^3H_6$
$5p_{3/2}5f_{5/2}(2)$	$5p5f\,{}^3D_2$						
$5p_{3/2}5f_{7/2}(2)$	$5p5f\,{}^1D_2$						

about 5%, while the ratio of the second and first ($E^{(2)}/E^{(1)}$) orders is much larger, 25%–35%. It should be noted that corrections for the frequency-dependent Breit interaction [36] are included in the first order only. The difference between the first-order Breit corrections calculated with and without frequency dependence is small, 1%–2%. The Breit corrections are smaller by a factor of 15–50 than the corresponding Coulomb corrections of the same order. The ratio of the first-order Breit corrections and the second-order Breit-Coulomb correction is almost equal to 1, while they have different signs and almost cancel each other in the case of Sm-like W^{12+}. The ratio of the first-order Breit correction and the second-order Breit-Coulomb correction slowly increases with increasing nuclear charge Z and and is equal to 2.5–3.0 for Sm-like uranium, U^{30+}.

The ratio of diagonal and nondiagonal matrix elements is about a factor of 3–10 larger than the first- and second-order contributions. The first-order nondiagonal matrix elements are symmetric, but the second-order nondiagonal matrix elements are not symmetric. The values of $E^{(2)}[v'w'(J),vw(J)]$ and $E^{(2)}[vw(J),v'w'(J)]$ matrix elements differ in some cases by a factor of 2–10 and occasionally have opposite signs.

TABLE II. Contributions to the $E[5l_{j_1}5l'_{j_2},5l_{j_3}5l'_{j_4}J=0]$ energy matrices before diagonalization for the Sm-like W^{12+} ion. $E^{(0)}$, $E^{(1)}$, and $E^{(2)}$ are the zeroth, first-, and second-order Coulomb contributions; $B^{(1)}$ and $B^{(2)}$ are the first- and second-order Breit-Coulomb corrections. Units: a.u.

$5l_{j_1}5l'_{j_2}$	$5l_{j_3}5l'_{j_4}$	$E^{(0)}$	$E^{(1)}$	$B^{(1)}$	$E^{(2)}$	$B^{(2)}$
$5s_{1/2}5s_{1/2}$	$5s_{1/2}5s_{1/2}$	−22.24097	0.91250	0.02844	−0.33232	−0.02441
$5p_{1/2}5p_{1/2}$	$5p_{1/2}5p_{1/2}$	−19.79919	0.86310	0.03586	−0.30076	−0.02234
$5p_{3/2}5p_{3/2}$	$5p_{3/2}5p_{3/2}$	−18.78066	0.90767	0.02276	−0.27518	−0.01924
$5d_{3/2}5d_{3/2}$	$5d_{3/2}5d_{3/2}$	−15.04692	0.80515	0.01467	−0.21222	−0.01542
$5d_{5/2}5d_{5/2}$	$5d_{5/2}5d_{5/2}$	−14.87664	0.83157	0.01148	−0.20960	−0.01506
$5s_{1/2}5s_{1/2}$	$5p_{3/2}5p_{3/2}$	0.0	−0.27290	−0.00008	0.08384	0.00026
$5p_{3/2}5p_{3/2}$	$5s_{1/2}5s_{1/2}$	0.0	−0.27290	−0.00008	0.05930	0.00032
$5s_{1/2}5s_{1/2}$	$5d_{5/2}5d_{5/2}$	0.0	0.12334	0.00005	−0.03455	−0.00006
$5d_{5/2}5d_{5/2}$	$5s_{1/2}5s_{1/2}$	0.0	0.12334	0.00005	−0.00863	−0.00222
$5p_{1/2}5p_{1/2}$	$5d_{5/2}5d_{5/2}$	0.0	−0.07654	−0.00002	0.00833	−0.00002
$5d_{5/2}5d_{5/2}$	$5p_{1/2}5p_{1/2}$	0.0	−0.07654	−0.00002	0.00459	0.00019
$5p_{3/2}5p_{3/2}$	$5d_{5/2}5d_{5/2}$	0.0	−0.29330	−0.00014	0.05872	0.00018
$5d_{5/2}5d_{5/2}$	$5p_{3/2}5p_{3/2}$	0.0	−0.29330	−0.00014	0.05066	−0.00127

TABLE III. Energies of the even-parity states with $J = 0$ in Sm-like W^{12+}. $E^{(0+1)} \equiv E^{(0)} + E^{(1)} + B^{(1)}$. Units: cm^{-1}.

Absolute energies						Excitation energies					
jj coupl.	$E^{(0+1)}$	$E^{(2)}$	$B^{(2)}$	E_{LS}	E_{tot}	$E^{(0+1)}$	$E^{(2)}$	$B^{(2)}$	E_{LS}	E_{tot}	LS coupl.
$5s_{1/2}5s_{1/2}$	−4683478	−68504	−5320	1428	−4755874	0	0	0	0	0	$5s^2\,{}^1S_0$
$5p_{1/2}5p_{1/2}$	−4151353	−65106	−4877	3	−4221332	532126	3398	443	−1425	534542	$5p^2\,{}^3P_0$
$5p_{3/2}5p_{3/2}$	−3915341	−61446	−4265	114	−3980938	768138	7058	1054	−1314	774936	$5p^2\,{}^1S_0$
$5d_{3/2}5d_{3/2}$	−3128649	−46203	−3367	−14	−3178234	1554829	22301	1952	−1442	1577640	$5d^2\,{}^3P_0$
$5d_{5/2}5d_{5/2}$	−3064091	−50659	−3345	20	−3118075	1619388	17845	1974	−1407	1637800	$5d^2\,{}^1S_0$

We now discuss how the final energy levels are obtained from the above contributions. To determine the first-order energies, we diagonalize the symmetric first-order effective Hamiltonian, including both Coulomb and Breit interactions. The first-order expansion coefficient $C^N[vw(J)]$ (often called a mixing coefficient) is the Nth eigenvector of the first-order effective Hamiltonian, and $E^{(1)}[N]$ is the corresponding eigenvalue. The resulting eigenvectors are used to determine the second-order Coulomb correction $E^{(2)}[N]$, the second-order Breit-Coulomb correction $B^{(2)}[N]$, and the QED correction $E_{LS}[N]$.

In Table III, we list the following contributions to the energies of five excited states in Sm-like W^{12+}: the sum of the zeroth and first-order energies $E^{(0+1)} = E^{(0)} + E^{(1)} + B^{(1)}$, the second-order Coulomb energy $E^{(2)}$, the second-order Breit-Coulomb correction $B^{(2)}$, the QED correction E_{LS}, and the sum of the above contributions E_{tot}. The Lamb shift E_{LS} is approximated as the sum of the one-electron self-energy and the first-order vacuum-polarization energy. The vacuum-polarization contribution is calculated from the Uehling potential using the results of Fullerton and Rinker [37]. The self-energy contribution is estimated for the s, $p_{1/2}$, and $p_{3/2}$ orbitals by interpolating among the values obtained by Mohr [38–40] using Coulomb wave functions. For this purpose, an effective nuclear charge Z_{eff} is obtained by finding the value of Z_{eff} required to give a Coulomb orbital with the same average $\langle r \rangle$ as the DHF orbital.

Energies listed in Table III under the heading "Absolute energies" are given relative to the $[Kr]4d^{10}4f^{14}$ core, while those listed under the heading "Excitation energies" are given relative to the $[Kr]4d^{10}4f^{14}5s^2\,{}^1S_0$ ground state. When starting calculations from relativistic DF wave functions, it is natural to use jj designations for uncoupled energy matrix elements; however, neither jj nor LS coupling describes the *physical* states properly. We find that the mixing coefficients are equal to 0.5–0.8. Therefore, in Table III, both jj and LS designations are given. As we discussed above, the correlation corrections are large and have to be included in order to obtain accurate energy values for the Sm-like W^{12+} ion.

In Table IV, we display excitation energies in Sm-like W^{12+} for the 35 even-parity states and the 32 odd-parity states. Our final RMBPT results (E_{tot}) are given in the "RMBPT2" column. To show the size of the correlation contribution, we also included the data evaluated in the first-order approximation in columns labeled "RMBPT1." These data are obtained as a sum of the $E^{(0)}$, $E^{(1)}$, and $B^{(1)}$ values (see explanation of Table III). These RMBPT1 values are often referred to as the multiconfiguration Dirac-Fock values [41]. The largest contribution of correlation effects is found to be for the $5s5p\,{}^3P_j$ levels. The difference in the RMBPT2 and RMBPT1 results for these three levels given in Table IV is about 3%–5%. It is smaller (1%–3%) in the RMBPT2 and RMBPT1 energies for other levels given in Table IV.

To further explore the cause of such disagreement, we include in Table IV the results for excitation energies in the W^{12+} ion, calculated in different approximations. We carried out additional calculations of the W^{12+} energies using the Hartree-Fock-relativistic method (COWAN code [42]). The following set of configurations: $[5s^2 + 5p^2 + 5d^2 + 5s5d + 5p5f + 5s6s + 5s6d + 5s6g + 5p6p + 5p6f]$ and $[5s5p + 5s5f + 5p5d + 5p5g + 5s6f + 5p6d + 5p6g]$ was used. The core-excited $4f^{13}5s^25p$, $4f^{13}5s5p5d$, $4f^{13}5s5p^2$, and $4f^{13}5s5p5f$ configurations are also included in the even- and odd-parity complexes. Results of our calculations are incorporated in Table IV in column "COWAN." It should be noted that the scaling of electrostatic integrals in the COWAN code allows to correct for correlation effects. In many systems, it leads to good agreement with experimental energies. We used the same scaling factor (0.85) for all electrostatic integrals. The 0.85 scaling factor was introduced for the first time by Fawcett *et al.* [43]. These authors explained that the 0.85 factor was found empirically to obtain results in good agreement with experiment.

The COWAN results are in better agreement with the RMBPT1 values (about 1% difference between the values). The differences of the COWAN results with our final RMBPT2 values is about 1%–5%. We note that second-order RMBPT has a general tendency to overestimate the correlation correction. Full all-order treatment, which may be carried out within the framework of the coupled-cluster approach, is needed for an improvement of accuracy. In the future, it may be possible to implement a hybrid configuration interaction + linearized coupled-cluster method [44] for two-particle states. This work provides a starting point for a further development of the theoretical methods for such a highly correlated relativistic system. The small difference between the COWAN and RMBPT1 values indicates that the correlation correction was not incorporated in the results obtained by the COWAN code.

Our RMBPT values presented in Table IV are the first *ab initio* values for the levels energy in W^{12+}. To the best of our knowledge, there are no experimental energy values for this ion.

The RMBPT1, RMBPT2, and COWAN values of the excitation energies for the 66 even- and odd-parity states are also evaluated for the Sm-like Re^{13+}, Os^{14+}, Ir^{15+}, Pt^{16+}, Au^{17+}, Ra^{26+}, and U^{30+} ions. The differences among the

TABLE IV. Energies (in cm^{-1}) of Sm-like W^{12+} given relative to the ground state. Energies of the odd- and even-parity states are calculated in first-order and second-order RMBPT (columns labeled RMBPT1 and RMBPT2, respectively) and the Hartree-Fock relativistic method implemented in COWAN code (column "COWAN").

jj coupl.	RMBPT1	RMBPT2	COWAN	*LS* coupl.	*jj* coupl.	RMBPT1	RMBPT2	COWAN	*LS* coupl.
$5s_{1/2}5s_{1/2}$	0	0	0	$5s^2\,^1S_0$	$5s_{1/2}5g_{9/2}$	1489333	1522722	1503391	$5s5g\,^3G_5$
$5s_{1/2}5p_{1/2}$	225378	237140	226886	$5s5p\,^3P_0$	$5s_{1/2}5g_{7/2}$	1489674	1522943	1503487	$5s5g\,^1G_4$
$5s_{1/2}5p_{1/2}$	243019	252360	242071	$5s5p\,^3P_1$	$5d_{3/2}5d_{5/2}$	1504612	1529381	1513569	$5s5g\,^3G_3$
$5s_{1/2}5p_{3/2}$	332606	348369	332894	$5s5p\,^3P_2$	$5s_{1/2}5g_{9/2}$	1501829	1529806	1512553	$5s5g\,^3G_4$
$5s_{1/2}5p_{3/2}$	394436	392166	390295	$5s5p\,^1P_1$	$5d_{5/2}5d_{5/2}$	1536109	1559671	1544094	$5d^2\,^3F_2$
$5p_{1/2}5p_{1/2}$	532126	534542	532140	$5p^2\,^3P_0$	$5p_{3/2}5f_{5/2}$	1541898	1569551	1552744	$5d^2\,^3F_3$
$5p_{1/2}5p_{3/2}$	619166	628243	623802	$5p^2\,^3P_1$	$5d_{3/2}5d_{5/2}$	1542805	1577180	1556749	$5d^2\,^1G_4$
$5p_{1/2}5p_{3/2}$	621224	634556	627570	$5p^2\,^1D_2$	$5d_{5/2}5d_{3/2}$	1554829	1577640	1561567	$5d^2\,^3P_0$
$5p_{3/2}5p_{3/2}$	718323	735575	725900	$5p^2\,^3P_2$	$5d_{3/2}5d_{5/2}$	1550615	1577919	1561213	$5d^2\,^1D_2$
$5s_{1/2}5d_{3/2}$	753922	767330	755687	$5s5d\,^3D_1$	$5p_{3/2}5f_{5/2}$	1553868	1579934	1563743	$5d^2\,^3F_4$
$5s_{1/2}5d_{3/2}$	760078	773522	761945	$5s5d\,^3D_2$	$5d_{3/2}5d_{5/2}$	1563179	1587067	1570500	$5d^2\,^3P_1$
$5p_{3/2}5p_{3/2}$	768138	774936	766355	$5p^2\,^1S_0$	$5p_{1/2}5f_{5/2}$	1573680	1598944	1580925	$5d^2\,^3P_2$
$5s_{1/2}5d_{5/2}$	771054	785580	773229	$5s5d\,^3D_3$	$5p_{3/2}5f_{7/2}$	1581137	1607952	1592873	$5p5f\,^1F_3$
$5s_{1/2}5d_{5/2}$	820724	820125	812408	$5s5d\,^1D_2$	$5p_{3/2}5f_{7/2}$	1589181	1613291	1598982	$5p5f\,^3G_5$
$5p_{1/2}5d_{3/2}$	997932	1022218	1009016	$5p5d\,^3F_2$	$5d_{5/2}5d_{5/2}$	1593059	1615364	1601278	$5p5f\,^3F_4$
$5p_{1/2}5d_{3/2}$	1047611	1057013	1050759	$5p5d\,^3D_1$	$5s_{1/2}5g_{7/2}$	1592744	1616806	1602373	$5p5f\,^3F_3$
$5p_{1/2}5d_{5/2}$	1035092	1057556	1044385	$5p5d\,^3F_3$	$5p_{3/2}5f_{5/2}$	1592805	1618084	1602298	$5p5f\,^3D_2$
$5p_{1/2}5d_{5/2}$	1042759	1058389	1048952	$5p5d\,^3P_2$	$5p_{3/2}5f_{5/2}$	1593821	1619649	1603653	$5p5f\,^3D_1$
$5p_{3/2}5d_{3/2}$	1121373	1143187	1131567	$5p5d\,^1D_2$	$5d_{5/2}5d_{5/2}$	1619388	1637800	1619330	$5d^2\,^1S_0$
$5p_{3/2}5d_{5/2}$	1115789	1147320	1129342	$5p5d\,^3F_4$	$5p_{3/2}5f_{7/2}$	1624257	1639762	1624992	$5p5f\,^1D_2$
$5p_{3/2}5d_{3/2}$	1131918	1151454	1140421	$5p5d\,^3D_3$	$5p_{3/2}5f_{7/2}$	1649083	1650455	1639786	$5p5f\,^1G_4$
$5p_{3/2}5d_{3/2}$	1136677	1153629	1144141	$5p5d\,^3P_0$	$5p_{1/2}5g_{7/2}$	1761229	1792544	1773994	$5p5g\,^3H_4$
$5p_{3/2}5d_{3/2}$	1139489	1155894	1146453	$5p5d\,^3P_1$	$5p_{1/2}5g_{9/2}$	1764673	1794934	1776784	$5p5g\,^3H_5$
$5p_{3/2}5d_{5/2}$	1148161	1165777	1155195	$5p5d\,^3P_2$	$5p_{1/2}5g_{9/2}$	1763858	1794986	1776640	$5p5g\,^3F_4$
$5p_{3/2}5d_{5/2}$	1162428	1182089	1170137	$5p5d\,^3D_3$	$5p_{1/2}5g_{7/2}$	1766739	1796888	1778097	$5p5g\,^3G_3$
$5p_{3/2}5d_{5/2}$	1197346	1206025	1195023	$5p5d\,^1P_1$	$5p_{3/2}5g_{7/2}$	1866493	1902535	1881719	$5p5g\,^1G_4$
$5s_{1/2}5f_{5/2}$	1210991	1231693	1218914	$5s5f\,^3F_2$	$5p_{3/2}5g_{7/2}$	1867810	1903572	1882775	$5p5g\,^3G_5$
$5s_{1/2}5f_{5/2}$	1213020	1233387	1220679	$5s5f\,^3F_3$	$5p_{3/2}5g_{9/2}$	1871520	1906056	1885432	$5p5g\,^3F_4$
$5s_{1/2}5f_{7/2}$	1215888	1235780	1223150	$5s5f\,^3F_4$	$5p_{3/2}5g_{9/2}$	1872715	1907151	1886821	$5p5g\,^3H_6$
$5s_{1/2}5f_{7/2}$	1250935	1254899	1246563	$5s5f\,^1F_3$	$5p_{3/2}5g_{7/2}$	1873618	1907308	1886624	$5p5g\,^3G_3$
$5p_{1/2}5f_{5/2}$	1459244	1491043	1473600	$5p5f\,^3G_3$	$5p_{3/2}5g_{9/2}$	1880755	1911786	1891772	$5p5g\,^1H_5$
$5p_{1/2}5f_{7/2}$	1460700	1494677	1475649	$5p5f\,^3G_4$	$5p_{3/2}5g_{7/2}$	1880435	1912546	1892027	$5p5g\,^3F_2$
$5d_{3/2}5d_{3/2}$	1474564	1501745	1485936	$5p5f\,^3F_2$	$5p_{3/2}5g_{9/2}$	1885452	1915148	1895165	$5p5g\,^1F_3$
$5p_{1/2}5f_{7/2}$	1478282	1503509	1488108	$5p5f\,^3D_3$					

results calculated in the three different approximations (i.e., the RMBPT1, RMBPT2, and COWAN codes) decreases with increasing nuclear charge Z of Sm-like ions. The largest difference is found for Sm-like U^{30+} and happens to be about 2% for the $5s5p\,^3P_J$ levels. A less than 1% difference is found for the other levels. Therefore, we estimate uncertainties of 1%–2% for the excitation energies of the 66 levels in Sm-like ions from $Z = 74$ up to $Z = 92$.

IV. *Z* DEPENDENCE OF EXCITATION ENERGIES AND MULTIPLET SPLITTING OF TRIPLET TERMS

Energies, relative to the ground state, of odd- and even-parity states with $J = 2$–5, divided by $(Z - 45)^2$, are shown in Figs. 2 and 3. It should be noted that Z was decreased by 45 to provide a better presentation of the energy plots. As in Tables III and IV, we use both *jj*- and *LS*-coupling designations. The limited number of energy levels is plotted to illustrate the change of mixing of levels belonging to different configurations with change of Z. We can observe such mixing for the levels of even-parity complexes with $J = 3$ and $J = 4$ in both panels of Fig. 2 and odd-parity complexes with $J = 2$ (left panel of Fig. 3) in the range $Z = 88$–89. The curve for the energy of the $5p5d\,^3P_2$ level almost crosses the curve for the $5s5f\,^3F_2$ level. The difference of energies between the two levels is equal to 108 00 cm^{-1} at $Z = 89$ (about 0.4% of the energy of these levels). A similar behavior of the curves for the $5d^2\,^3F_3$ and $5s5g\,^3G_3$ levels (left panel of Fig. 2) and $5d^2\,^1G_4$ and $5s5g\,^3G_4$ levels (right panel of Fig. 2) is observed.

It is known that the crossing of energy levels inside a complex with fixed J is forbidden by the Wigner and Neumann theorem (see, for example, Ref. [45]). We can observe from the left panel of Fig. 3 that the curves describing the energy of the $5p5d\,^3P_2$ and $5s5f\,^3F_2$ levels do not cross at $Z = 89$ and that the curve "5" stays above the curve "4" for the entire range of $Z = 74$–100. A similar behavior for the curves describing the energy of the $5d^2\,^3F_3$ and $5s5g\,^3G_3$ levels (the curves "2" and "3" in left panel of Fig. 2) and $5d^2\,^1G_4$ and $5s5g\,^3G_4$ levels

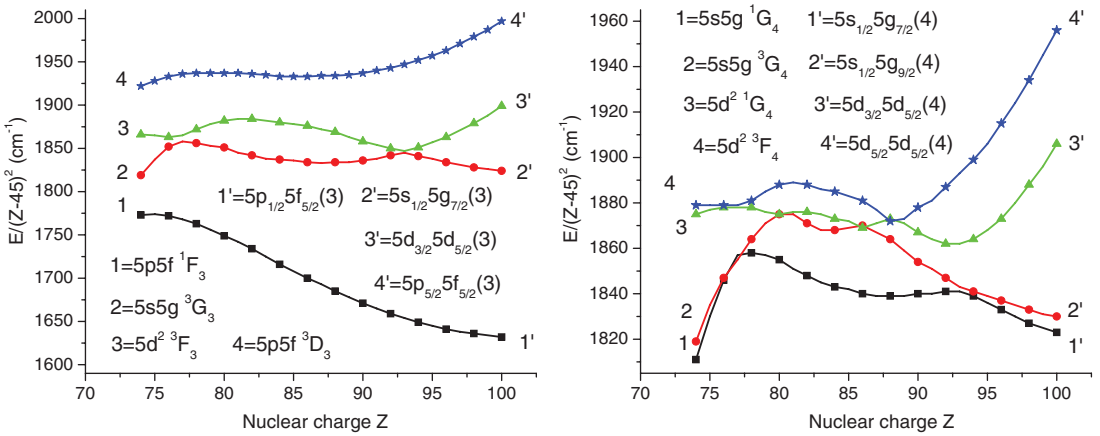

FIG. 2. (Color online) Z dependence of the even-parity energy levels $E/(Z-45)^2$ for Sm-like ions.

(the curves "2" and "3" in right panel of Fig. 2) may also be observed. Additionally, it should be noted that the curves describing the energy of the $5p5g\,^3H_5$ and $5p5g\,^1G_5$ levels (right panel of Fig. 3) are almost coincident with each other. The difference in energies between the two levels is about 0.5% for the entire Z interval.

It should be noted that the LS designations were chosen based upon small values of the multiplet splitting for low-Z ions. To confirm those designations, we obtained the fine-structure splitting for the even-parity $5s5d\,^3D$, $5p^2\,^3P$, $5d^2[^3P,^3F]$, $5p5f[^3D,^3F,^3G]$, and $5s5g\,^3G$ states and odd-parity $5s5p\,^3P$, $5s5f\,^3F$, $5p5d[^3P,^3D,^3F]$, and $5p5g[^3D,^3F,\,^3G,^3H]$ states.

Energy differences between levels of even- and odd-parity triplet terms, divided by $(Z-45)^2$, are illustrated in Fig. 4. The energy intervals for the $5p5g(^3F_3–^3F_2)$, $5p5g(^3F_4–^3F_3)$, $5p5g(^3G_4–^3G_3)$, and $5p5g(^3G_5–^3G_4)$ states almost do not change with Z, as can be seen from the bottom left panel of Fig. 4. There is a very sharp change of splitting around $Z=89$ in the curves describing the $5s5f(^3F_3–^3F_2)$ and $5s5f(^3F_4–^3F_3)$ splitting, but the energies $\Delta E/(Z-45)^2$ change by only a small amount, from -40 to 40 cm^{-1}. A similar behavior of the curves is observed for the $5s5d(^3D_2–^3D_1)$ and $5s5d(^3D_3–^3D_2)$ intervals displayed on the top left panel of Fig. 4. The energy intervals vary strongly with Z for the $5p5g(^3F_3–^3F_2)$, $5p5g(^3F_4–3F_3)$, and $5p5g(^3G_4–^3G_3)$ intervals. The triplet splitting for the $5s5d\,^3D$, $5d^2[^3P,^3F]$, and $5p5f[^3D,^3F,^3G]$ terms change in the small range of -12–12 cm^{-1} in units of $(Z-45)^2$ cm^{-1}, which amounts to 0.2%–0.5% of the energy of those terms. Our calculations show that the fine structures of almost all the levels illustrated in Fig. 4 do not follow the Landé rules even for small Z. The unusual splitting may be caused by changes from LS to jj coupling, with mixing from other triplet and singlet states. The different J states are mixed differently. Further experimental confirmation would be very helpful in verifying the correctness of these, sometimes sensitive, mixing parameters.

V. DIPOLE MATRIX ELEMENTS, LINE STRENGTHS, OSCILLATOR STRENGTHS, AND TRANSITION RATES IN Sm-LIKE IONS

We designate the first-order dipole matrix element by $Z^{(1)}$, the Coulomb correction to the second-order matrix element by $Z^{(2)}$, and the second-order Breit correction by $B^{(2)}$. The evaluation of $Z^{(1)}$, $Z^{(2)}$, and $B^{(2)}$ for Sm-like ions ions follows the pattern of the corresponding calculation for Be- and Zn-like ions in Refs. [26,32]. These matrix elements are calculated in both length and velocity gauges. The differences between length and velocity forms are illustrated for the uncoupled

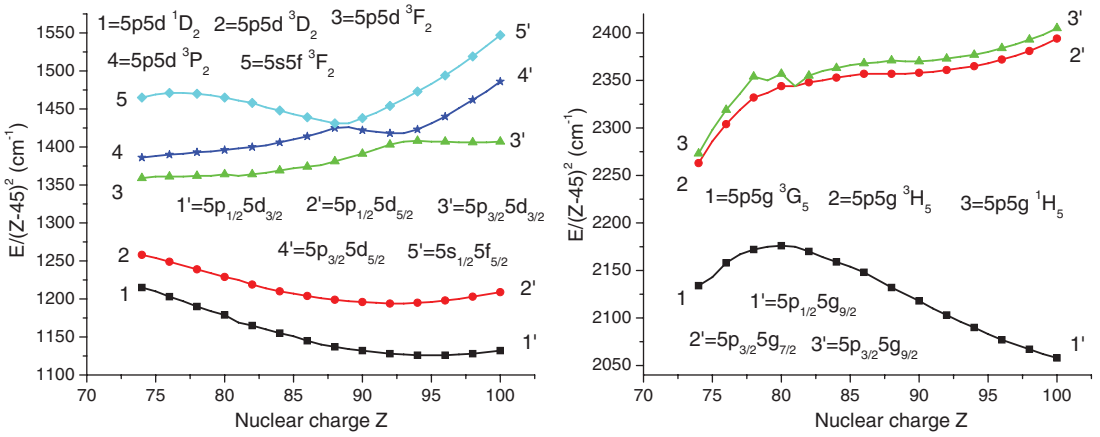

FIG. 3. (Color online) Z dependence of the odd-parity energy levels $E/(Z-45)^2$ for Sm-like ions.

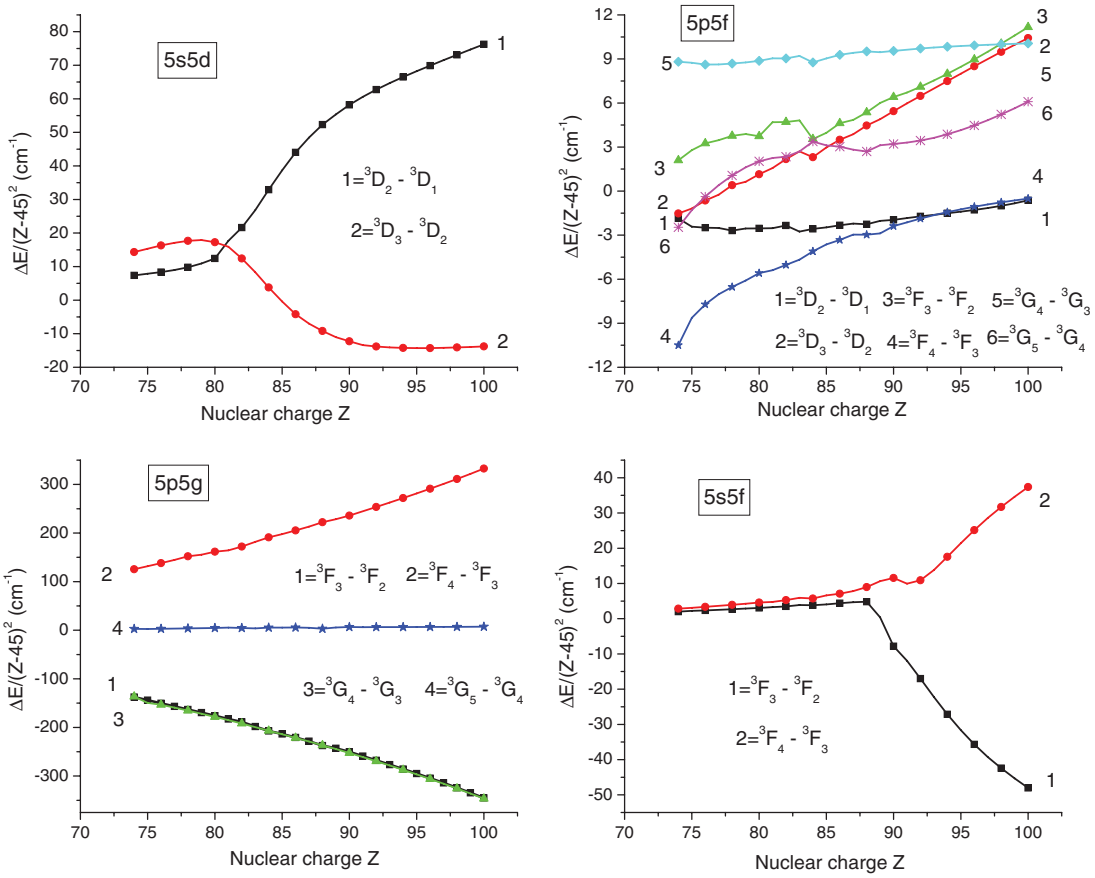

FIG. 4. (Color online) Energy splitting [$\Delta E/(Z-45)^2$ in cm^{-1}] for triplet terms as a function of Z for Sm-like ions.

$5s_{1/2}5s_{1/2}(0)$-$5s_{1/2}5p_{3/2}(1)$ matrix element in Fig. 5. It should be noted, that the second-order Coulomb and Breit matrix elements are multiplied by a factor of 10 and 100, respectively ($10 \times Z^{(2)}$ and $100 \times B^{(2)}$), in order to show them on the same scale as the first-order Coulomb matrix element $Z^{(1)}$. The contributions of the second-order matrix elements $Z^{(2)}$ and $B^{(2)}$ are much larger in velocity form than in length form and have different signs (compare curves describing $Z^{(2)}$ and $B^{(2)}$ in the two panels of Fig. 5). The differences between length and velocity form are compensated by "derivative terms" $P^{(\mathrm{derv})}$ [26,32], as shown later.

A. Example: Dipole matrix elements, line strengths, oscillator strengths, and transition rates in Sm-like W^{12+}

In Table V, we list the values of the *uncoupled* first- and second-order dipole matrix elements $Z^{(1)}$, $Z^{(2)}$, and $B^{(2)}$, together with the derivative terms $P^{(\mathrm{derv})}$ for Sm-like tungsten, $Z = 74$. For simplicity, we only list values for the nine dipole transitions between even-parity states with $J = 0$ $(5s_{1/2}5s_{1/2} + 5p_{1/2}5p_{1/2} + 5p_{3/2}5p_{3/2}5d_{3/2}5d_{3/2} + 5d_{5/2}5d_{5/2})$ and odd-parity states with $J = 1$ $(5s_{1/2}5p_{1/2} + 5s_{1/2}5p_{3/2} + 5p_{1/2}5d_{3/2} + 5p_{3/2}5d_{3/2} + 5p_{3/2}5d_{5/2})$. The derivative terms shown in Table V arise because transition amplitudes depend on energy, and the transition energy changes order by order in RMBPT calculations. Both length (L) and velocity (V) forms are given for the matrix elements. The first-order matrix elements $Z_L^{(1)}$ and $Z_V^{(1)}$ differ by only 1%–2%; the L-V differences between second-order matrix elements are much larger (10%–20%) as seen by comparing $Z_L^{(2)}$ and $Z_V^{(2)}$. It should be noted that the first-order matrix elements $Z_L^{(1)}$ and $Z_V^{(1)}$ are not zero for the ten matrix elements $5s_{1/2}5s_{1/2}(0)$–$5s_{1/2}5p_{1/2}(1)$, $5s_{1/2}5s_{1/2}(0)$–$5s_{1/2}5p_{3/2}(1)$, $5p_{1/2}5p_{1/2}(0)$–$5s_{1/2}5p_{1/2}(1)$, $5p_{1/2}5p_{1/2}(0)$–$5p_{1/2}5d_{3/2}(1)$, $5p_{3/2}5p_{3/2}(0)$–$5s_{1/2}5p_{3/2}(1)$, $5p_{3/2}5p_{3/2}(0)$–$5p_{3/2}5d_{3/2}(1)$, $5p_{3/2}5p_{3/2}(0)$–$5p_{3/2}5d_{5/2}(1)$, $5d_{3/2}5d_{3/2}(0)$–$5p_{1/2}5d_{3/2}(1)$, $5d_{3/2}5d_{3/2}(0)$–$5p_{3/2}5d_{3/2}(1)$, and $5d_{5/2}5d_{5/2}(0)$–$5p_{3/2}5d_{5/2}(1)$ when a one-electron transition is taking place. The other four transitions $[5s_{1/2}5s_{1/2}(0)$–$5p_{1/2}5d_{3/2}(1)$, $(5s_{1/2}5s_{1/2}(0)$–$5p_{3/2}5d_{5/2}(1)$, $5d_{3/2}5d_{3/2}(0)$–$5s_{1/2}5p_{3/2}(1)$, and $5d_{5/2}5d_{5/2}(0)$–$5p_{1/2}5d_{3/2}(1)]$ are two-electron transitions and nonzero contributions only start from the second-order diagrams. We can see from Table V that those four matrix elements $Z_L^{(2)}$ and $Z_V^{(2)}$ are smaller than the ten one-electron contributions. It is also seen from Table V, that $P^{(\mathrm{derv})}$ in length form almost equals $Z^{(1)}$ in length form but $P^{(\mathrm{derv})}$ in velocity form is smaller than $Z^{(1)}$ in velocity form by five to six orders of magnitude.

Values of *coupled* reduced matrix elements [26,32] in length and velocity forms are given in Table VI for some of the transitions considered in Table V. Although we use an intermediate-coupling scheme, it is nevertheless convenient to label the physical states using the LS scheme. Both designations are given in Table VI. The L and V forms of the coupled matrix elements in Table VI differ only in the

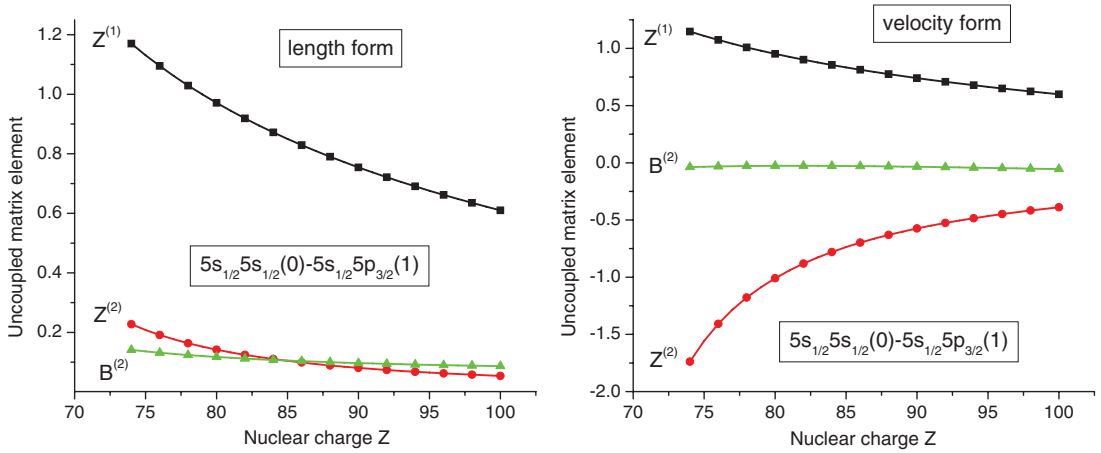

FIG. 5. (Color online) Uncoupled matrix elements for the $5s_{1/2}5s_{1/2}(0) - 5s_{1/2}5p_{3/2}(1)$ transition calculated in length and velocity forms for Sm-like ions.

fourth or fifth digits. These L-V differences arise because we start our RMBPT calculations using a nonlocal Dirac-Fock (DF) potential. If we were to replace the DF potential by a local potential, the differences would disappear completely. The next source of L-V differences arises from a noncomplete model space as was used for the Be-like system in Ref. [26] and for the Zn-like system in Ref. [32]. The last two columns in Table VI show L and V values of coupled reduced matrix elements calculated without the second-order contribution. As is seen from this table, removing the second-order contribution increases the L-V differences. We also see that the values of the coupled reduced matrix elements calculated in the first-order and second-order approximations are substantially different. The second-order contribution leads to a change of the coupled reduced matrix element by a factor of 2–4 (compare the values of the $5s5s\ ^1S_0$–$5p5d\ ^3P_1$ matrix element given in the first line of Table VI).

We combine the RMBPT energies given in column "RMBPT2" of Table IV and our RMBPT values of the dipole matrix elements listed in Table VI to calculate weighted transition rates gA_r and weighted oscillator strengths gf [26,32]. The value of the line strengths S are obtained as a square of the dipole matrix elements. The complete list of transitions consists of 567 transitions. A limited number of transitions was presented in Table VII. In this table, we display wavelengths, line strengths, weighted oscillator strengths, and weighted transition rates for the dipole transitions in Sm-like W^{12+} calculated by the RMBPT code. The transitions are ordered by wavelength.

To check the accuracy of our RMBPT values, we carried out additional calculations of the line strengths, oscillator strengths, and transition rates in the W^{12+} ion using the Hartree-Fock-relativistic method (COWAN code [42]). We implemented the same set of configurations mentioned in Sec. III. We did not display the COWAN values, however, but listed our S, gf, and gA_r values according to the level of disagreement with results from the COWAN code.

In the left column of Table VII, we display S, gf, and gA_r values for 40 transitions. It is found that correlation corrections for these transitions contribute about 10%–20%. As a result, the differences between the S, gf, and gA_r values obtained by the RMBPT and COWAN codes is also less than 20%.

TABLE V. Uncoupled reduced matrix elements in length L and velocity V forms for even-odd parity transitions in Sm-like W^{12+}.

Even parity	Odd parity	$Z_L^{(1)}$	$Z_V^{(1)}$	$Z_L^{(2)}$	$Z_V^{(2)}$	$B_L^{(2)}$	$B_V^{(2)}$	$P_L^{(\mathrm{derv})}$	$P_V^{(\mathrm{derv})}$
$5s_{1/2}5s_{1/2}(0)$	$5s_{1/2}5p_{1/2}(1)$	−0.82059	−0.81332	0.13720	0.12900	−0.00117	−0.00301	−0.82060	−0.00003
$5s_{1/2}5s_{1/2}(0)$	$5s_{1/2}5p_{3/2}(1)$	−1.16966	−1.14737	0.19322	0.17384	−0.00141	0.00038	−1.16958	0.00011
$5p_{1/2}5p_{1/2}(0)$	$5s_{1/2}5p_{1/2}(1)$	0.82059	0.81332	−0.13851	−0.11527	0.00117	0.00311	0.82060	0.00003
$5p_{1/2}5p_{1/2}(0)$	$5p_{1/2}5d_{3/2}(1)$	1.23664	1.21803	−0.18846	−0.17802	0.00244	−0.00334	1.23654	−0.00007
$5p_{3/2}5p_{3/2}(0)$	$5s_{1/2}5p_{3/2}(1)$	0.82708	0.81131	−0.14244	−0.13054	0.00102	−0.00019	0.82702	−0.00008
$5p_{3/2}5p_{3/2}(0)$	$5p_{3/2}5d_{3/2}(1)$	0.41406	0.41029	−0.05797	−0.06031	0.00056	−0.00069	0.41406	0.00005
$5p_{3/2}5p_{3/2}(0)$	$5p_{3/2}5d_{5/2}(1)$	−1.24186	−1.22907	0.17343	0.18169	−0.00166	0.00248	−1.24173	0.00018
$5d_{3/2}5d_{3/2}(0)$	$5p_{1/2}5d_{3/2}(1)$	−0.87444	−0.86128	0.08012	0.06809	−0.00153	0.00249	−0.87437	0.00005
$5d_{3/2}5d_{3/2}(0)$	$5p_{3/2}5d_{3/2}(1)$	−0.41406	−0.41029	0.05629	0.05123	−0.00059	0.00061	−0.41406	−0.00005
$5d_{5/2}5d_{5/2}(0)$	$5p_{3/2}5d_{5/2}(1)$	1.01398	1.00353	−0.13401	−0.11325	0.00171	−0.00162	1.01387	−0.00015
$5s_{1/2}5s_{1/2}(0)$	$5p_{1/2}5d_{3/2}(1)$	0.0	0.0	−0.00606	0.00206	−0.00001	−0.00001	0.0	0.0
$5s_{1/2}5s_{1/2}(0)$	$5p_{3/2}5d_{5/2}(1)$	0.0	0.0	0.01040	−0.00128	0.00002	0.00002	0.0	0.0
$5d_{3/2}5d_{3/2}(0)$	$5s_{1/2}5p_{3/2}(1)$	0.0	0.0	0.00671	0.00558	−0.00006	−0.00007	0.0	0.0
$5d_{5/2}5d_{5/2}(0)$	$5p_{1/2}5d_{3/2}(1)$	0.0	0.0	−0.01416	−0.01086	0.00000	0.00000	0.0	0.0

TABLE VI. Coupled reduced matrix elements calculated in length L and velocity V forms for Sm-like W^{12+}.

		First order		RMBPT			
$l_1 l_2\ LSJ$	$l_3 l_4\ L'S'J'$	L	V	L	V	$j_1 j_2\ (J)$	$j_3 j_4\ (J')$
$5s5s\ ^1S_0$	$5p5d\ ^3P_1$	0.00289	0.00275	0.00896	0.00895	$5s_{1/2}5s_{1/2}(0)$	$5p_{3/2}5d_{3/2}(1)$
$5p5f\ ^3D_1$	$5s5f\ ^3F_2$	1.00043	0.97884	0.85945	0.86189	$5p_{3/2}5f_{5/2}(1)$	$5s_{1/2}5f_{5/2}(2)$
$5p5f\ ^1D_2$	$5p5d\ ^1D_2$	0.10459	0.10273	0.10414	0.10398	$5p_{3/2}5f_{7/2}(2)$	$5p_{1/2}5d_{3/2}(2)$
$5p5p\ ^1D_2$	$5p5g\ ^1F_3$	0.00340	0.00384	0.00162	0.00167	$5p_{3/2}5p_{3/2}(2)$	$5p_{3/2}5g_{9/2}(3)$
$5d5d\ ^3P_2$	$5s5f\ ^3F_3$	0.31381	0.30862	0.26790	0.26856	$5d_{3/2}5d_{5/2}(2)$	$5s_{1/2}5f_{5/2}(3)$
$5p5f\ ^1F_3$	$5p5d\ ^1D_2$	1.84039	1.81587	1.64349	1.65378	$5p_{1/2}5f_{5/2}(3)$	$5p_{1/2}5d_{3/2}(2)$
$5p5f\ ^1F_3$	$5s5f\ ^3F_2$	0.14950	0.17818	0.35983	0.36462	$5p_{1/2}5f_{5/2}(3)$	$5s_{1/2}5f_{5/2}(2)$
$5p5f\ ^1F_3$	$5p5g\ ^3G_4$	2.05805	2.09667	2.12967	2.13281	$5p_{1/2}5f_{5/2}(3)$	$5p_{1/2}5g_{7/2}(4)$
$5p5f\ ^3F_3$	$5s5f\ ^3F_4$	1.13078	1.11839	0.98857	0.99472	$5p_{1/2}5f_{7/2}(3)$	$5s_{1/2}5f_{7/2}(4)$
$5p5f\ ^3G_3$	$5s5f\ ^3F_4$	0.56143	0.54984	0.47535	0.47943	$5p_{3/2}5f_{7/2}(3)$	$5s_{1/2}5f_{7/2}(4)$
$5p5f\ ^3F_4$	$5p5d\ ^1D_3$	0.04889	0.05931	0.11262	0.12113	$5p_{1/2}5f_{7/2}(4)$	$5p_{3/2}5d_{5/2}(3)$
$5d5d\ ^1G_4$	$5s5f\ ^1F_3$	0.08073	0.07186	0.12338	0.11687	$5d_{3/2}5d_{5/2}(4)$	$5s_{1/2}5f_{7/2}(3)$
$5s5g\ ^3G_5$	$5p5g\ ^3H_6$	1.11495	1.06403	1.10495	1.10614	$5s_{1/2}5g_{9/2}(5)$	$5p_{3/2}5g_{9/2}(6)$

TABLE VII. Wavelengths (λ in Å), line strengths (S in a.u.), weighted oscillator strengths (gf), and weighted transition rates (gA_r in 1/s) for transitions in Sm-like W^{12+} calculated by the RMBPT code.

Transitions		λ	S		gA_r	Transitions		λ	S		gA_r
$l_1 l_2\ LSJ$	$l_3 l_4\ L'S'J'$	Å	a.u.	gf	1/s	$l_1 l_2\ LSJ$	$l_3 l_4\ L'S'J'$	Å	a.u.	gf	1/s
$5p5f\ ^1D_2$	$5s5p\ ^1P_1$	80.154	7.67[−5]	2.91[−4]	3.02[08]	$5p^2\ ^1D_2$	$5s5f\ ^3F_2$	167.466	1.61[−3]	2.92[−3]	6.94[08]
$5p5f\ ^1D_2$	$5p5d\ ^3F_2$	161.932	1.08[−2]	2.03[−2]	5.17[09]	$5p5f\ ^1D_2$	$5p5d\ ^3P_2$	172.007	3.72[−2]	6.57[−2]	1.48[10]
$5d^2\ ^1S_0$	$5p5d\ ^3D_1$	172.180	4.17[−2]	7.36[−2]	1.66[10]	$5p5f\ ^3F_3$	$5p5d\ ^3F_3$	178.811	2.90[−2]	4.93[−2]	1.03[10]
$5p5f\ ^3D_2$	$5p5d\ ^3D_1$	178.231	1.47[−2]	2.50[−2]	5.25[09]	$5p5f\ ^3D_3$	$5p5d\ ^3F_2$	207.775	3.64[−2]	5.32[−2]	8.22[09]
$5d^2\ ^3P_2$	$5p5d\ ^3F_3$	184.710	5.15[−2]	8.48[−2]	1.66[10]	$5p5f\ ^3F_2$	$5p5d\ ^3F_2$	208.539	8.86[−1]	1.29[0]	1.98[11]
$5d^2\ ^3P_2$	$5p5d\ ^3P_2$	184.995	1.90[−1]	3.12[−1]	6.08[10]	$5p5f\ ^3D_1$	$5p5d\ ^3P_0$	214.583	8.14[−1]	1.15[0]	1.67[11]
$5s5d\ ^3D_1$	$5s5p\ ^3P_0$	188.612	5.13[−1]	8.26[−1]	1.55[11]	$5p5f\ ^1F_3$	$5p5d\ ^1D_2$	215.163	3.40[0]	4.81[0]	6.93[11]
$5p^2\ ^1S_0$	$5s5p\ ^3P_1$	191.360	6.51[−3]	1.03[−2]	1.88[09]	$5s5d\ ^3D_1$	$5s5f\ ^3F_2$	215.349	2.58[0]	3.65[0]	5.24[11]
$5d^2\ ^3F_4$	$5p5d\ ^3F_3$	191.432	1.45[0]	2.31[0]	4.20[11]	$5p5f\ ^3D_1$	$5p5d\ ^3P_1$	215.631	8.44[−1]	1.19[0]	1.71[11]
$5p5f\ ^1G_4$	$5p5d\ ^3D_3$	192.447	9.45[−1]	1.49[0]	2.69[11]	$5p5f\ ^3D_2$	$5p5d\ ^3P_1$	216.361	1.85[0]	2.60[0]	3.71[11]
$5s5d\ ^3D_1$	$5s5p\ ^3P_1$	194.186	3.54[−1]	5.54[−1]	9.80[10]	$5p5f\ ^3D_2$	$5p5d\ ^3P_2$	221.089	1.38[0]	1.90[0]	2.59[11]
$5s5g\ ^3G_3$	$5p5d\ ^3F_2$	197.175	4.74[−1]	7.30[−1]	1.25[11]	$5p5f\ ^3F_3$	$5p5d\ ^3P_2$	221.715	3.73[0]	5.11[0]	6.93[11]
$5d^2\ ^3F_2$	$5p5d\ ^3D_1$	198.942	2.30[0]	3.52[0]	5.93[11]	$5p^2\ ^3P_2$	$5p5d\ ^3D_3$	223.957	3.05[0]	4.14[0]	5.51[11]
$5p5f\ ^3F_3$	$5p5d\ ^3D_3$	214.891	5.54[−1]	7.83[−1]	1.13[11]	$5p5f\ ^3D_3$	$5p5d\ ^3P_2$	224.659	3.14[0]	4.25[0]	5.62[11]
$5p5f\ ^3D_1$	$5p5d\ ^3P_2$	220.326	9.79[−2]	1.35[−1]	1.85[10]	$5p5f\ ^3F_3$	$5p5d\ ^3D_3$	230.035	8.41[−1]	1.11[0]	1.40[11]
$5d^2\ ^3P_2$	$5p5d\ ^3P_1$	225.708	7.30[−1]	9.82[−1]	1.29[11]	$5p5f\ ^1D_2$	$5p5d\ ^1P_1$	230.554	4.02[0]	5.29[0]	6.64[11]
$5p5f\ ^3F_4$	$5p5d\ ^3D_3$	230.800	2.64[0]	3.48[0]	4.35[11]	$5d^2\ ^3P_1$	$5p5d\ ^3P_0$	230.714	6.25[−1]	8.23[−1]	1.03[11]
$5p^2\ ^1D_2$	$5p5d\ ^3D_1$	236.710	7.99[−3]	1.02[−2]	1.22[09]	$5d^2\ ^3P_1$	$5p5d\ ^3P_1$	231.925	6.39[−1]	8.37[−1]	1.04[11]
$5p5f\ ^3G_3$	$5p5g\ ^3F_4$	240.956	2.02[−2]	2.55[−2]	2.93[09]	$5p^2\ ^1S_0$	$5p5d\ ^1P_1$	231.971	1.21[0]	1.59[0]	1.97[11]
$5p5f\ ^3G_3$	$5p5g\ ^1G_4$	243.018	1.31[−1]	1.64[−1]	1.85[10]	$5p^2\ ^3P_1$	$5p5d\ ^3D_1$	233.225	1.74[−1]	2.27[−1]	2.78[10]
$5p5f\ ^3G_4$	$5p5g\ ^3G_5$	244.562	1.52[−1]	1.89[−1]	2.11[10]	$5d^2\ ^3P_0$	$5p5d\ ^3P_1$	237.110	1.66[−1]	2.12[−1]	2.52[10]
$5p5f\ ^3G_4$	$5p5g\ ^1G_4$	245.183	1.60[−2]	1.99[−2]	2.21[09]	$5s5d\ ^3D_1$	$5s5p\ ^3P_2$	238.686	3.14[−2]	4.00[−2]	4.68[09]
$5s5g\ ^1G_4$	$5p5d\ ^3D_3$	269.187	1.32[0]	1.49[0]	1.37[11]	$5d^2\ ^3F_3$	$5p5d\ ^3D_3$	239.179	3.66[−1]	4.65[−1]	5.42[10]
$5s5d\ ^3D_3$	$5p5d\ ^3F_4$	276.442	8.19[−1]	8.99[−1]	7.85[10]	$5d^2\ ^1D_2$	$5p5d\ ^3D_3$	252.634	2.56[−2]	3.08[−2]	3.22[09]
$5s5g\ ^3G_4$	$5p5d\ ^3D_3$	288.561	1.94[0]	2.04[0]	1.63[11]	$5p^2\ ^1D_2$	$5p5d\ ^3F_2$	257.957	3.15[−1]	3.71[−1]	3.72[10]
$5d^2\ ^3F_3$	$5p5g\ ^3G_3$	296.071	7.64[−2]	7.84[−2]	5.97[09]	$5s5g\ ^1G_4$	$5p5g\ ^3G_5$	262.723	2.11[−1]	2.44[−1]	2.36[10]
$5p5f\ ^3D_3$	$5p5d\ ^3P_2$	296.093	7.28[−3]	7.47[−3]	5.68[08]	$5p5f\ ^1F_3$	$5s5f\ ^3F_2$	265.774	1.30[0]	1.48[0]	1.40[11]
$5d^2\ ^3F_2$	$5s5f\ ^3F_2$	304.898	5.50[−3]	5.48[−3]	3.93[08]	$5p5f\ ^3D_3$	$5p5d\ ^3D_3$	284.047	4.10[−2]	4.38[−2]	3.62[09]
$5d^2\ ^3F_4$	$5p5g\ ^3G_5$	308.987	2.23[0]	2.19[0]	1.53[11]	$5p5f\ ^3D_3$	$5p5d\ ^3D_3$	294.474	6.29[−2]	6.49[−2]	4.99[09]
$5p5f\ ^3G_4$	$5p5g\ ^3H_4$	335.720	2.02[−1]	1.83[−1]	1.08[10]	$5d^2\ ^1G_4$	$5p5g\ ^1H_5$	298.859	3.72[0]	3.78[0]	2.83[11]
$5p5f\ ^3F_3$	$5p5g\ ^3F_2$	338.135	1.06[−1]	9.51[−2]	5.55[09]	$5p5f\ ^3G_3$	$5p5g\ ^3G_3$	326.963	7.13[−1]	6.63[−1]	4.13[10]
$5p5f\ ^1F_3$	$5p5g\ ^1G_4$	343.080	9.44[0]	8.36[0]	4.74[11]	$5p5f\ ^3G_4$	$5p5g\ ^3F_4$	332.990	7.82[−1]	7.13[−1]	4.29[10]
$5p5f\ ^3F_4$	$5p5g\ ^3F_4$	344.007	7.97[−1]	7.04[−1]	3.97[10]	$5p5f\ ^3G_5$	$5p5g\ ^1H_5$	335.014	8.08[−2]	7.33[−2]	4.36[09]
$5p5f\ ^3G_5$	$5p5g\ ^3G_5$	344.494	7.17[−1]	6.32[−1]	3.55[10]	$5s5g\ ^3G_3$	$5s5f\ ^3F_3$	337.845	9.95[−1]	8.95[−1]	5.23[10]
$5p5f\ ^1G_4$	$5p5g\ ^1H_5$	382.656	9.76[0]	7.75[0]	3.53[11]	$5p5f\ ^3D_2$	$5p5g\ ^3F_2$	339.602	1.20[0]	1.07[0]	6.20[10]
$5p5f\ ^1G_4$	$5p5g\ ^3F_4$	391.235	1.00[−1]	7.78[−2]	3.39[09]	$5p5f\ ^3G_5$	$5p5g\ ^3H_6$	340.298	1.71[1]	1.53[1]	8.82[11]
$5p^2\ ^3P_1$	$5s5p\ ^1P_1$	423.591	3.76[−2]	2.69[−2]	1.00[09]	$5p5f\ ^3G_5$	$5p5g\ ^3F_4$	341.571	1.94[−1]	1.73[−1]	9.87[09]
$5s5d\ ^1D_2$	$5p5d\ ^3F_2$	494.822	4.17[−2]	2.56[−2]	6.97[08]	$5p5f\ ^3F_4$	$5p5g\ ^3G_3$	342.531	1.41[−1]	1.25[−1]	7.09[09]
$5p5f\ ^3F_3$	$5p5g\ ^3H_4$	569.029	2.88[−3]	1.54[−3]	3.17[07]	$5p^2\ ^3P_0$	$5s5p\ ^3P_1$	354.381	4.47[−1]	3.83[−1]	2.04[10]
$5p5f\ ^1G_4$	$5p5g\ ^3H_5$	692.142	5.39[−1]	2.37[−1]	3.29[09]	$5s5g\ ^3G_3$	$5p5g\ ^3H_4$	379.993	5.33[0]	4.26[0]	1.97[11]

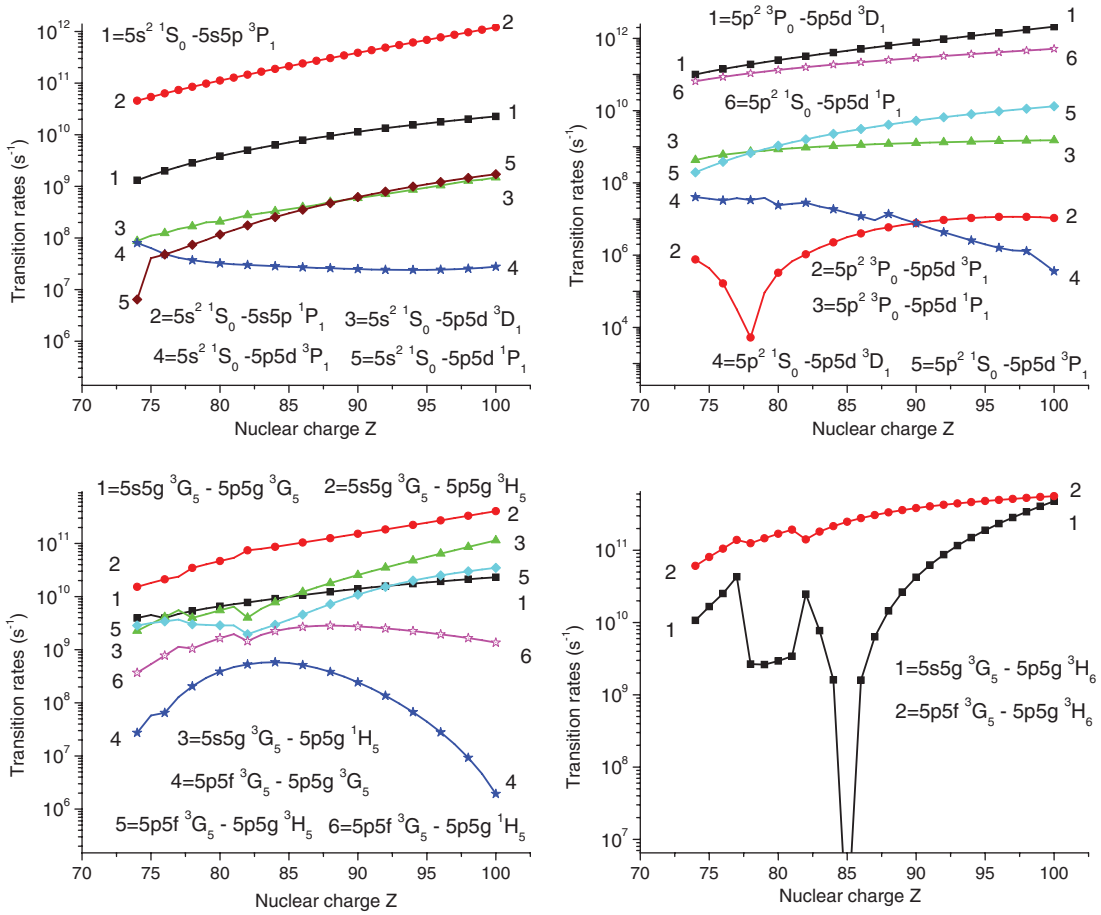

FIG. 6. (Color online) Transition rates for even-odd transitions in Sm-like ions as a function of Z.

In the second column of Table VII, we present another 40 transitions. There is substantially larger disagreement (20%–40%) between the RMBPT and COWAN results for S, gf, and gA_r properties observed. However, the COWAN results for S, gf, and gA_r values are in better agreement (about 10%) with the results obtained in the first-order RMBPT1 approximation. Those S, gf, and gA_r RMBPT1 values are evaluated by combining the RMBPT energies given in column "RMBPT1" of Table IV and the values of the dipole matrix elements listed in column "First order" of Table VI.

B. Z dependence of transition rates in Sm-like ions

The general trends of the Z dependence of the transition rates for the $5l_15l_2\,^{1,3}L_J$–$5l_35l_4\,^{1,3}L'_{J'}$ lines are presented in Figs. 6 and 7. In these figures, we show transitions to a fixed J state from states belonging to a limited set of the $5l5l'\,^{1,3}L_J$ states, i.e., a *complex* of states. A complex includes all states of the same parity and J obtained from the combinations of the $5l5l'\,^{1,3}L_J$ states. For example, the odd-parity complex with $J=1$ includes the states $5s5p\,^{1,3}P_1$, $5p5d\,^3D_1$, and $5p5d\,^{1,3}P_1$ in LS coupling or $5s_{1/2}5p_{1/2}(1)$, $5s_{1/2}5p_{3/2}(1)$, $5p_{1/2}5d_{3/2}(1)$, $5p_{3/2}5d_{3/2}(1)$, and $5p_{3/2}5d_{5/2}(1)$ in jj coupling. Later, we use the LS designations since they are more conventional.

In the two top panels of Fig. 6, we present a limited set (11 of the 25 transitions included in even-parity complex with $J=0$ and odd-parity complexes with $J=1$) of transition rates for the $5s^2\,^1S_0$–$5s5p\,^{1,3}P_1$, $5s^2\,^1S_0$–$5p5d\,^{1,3}P_1$, $5s^2\,^1S_0$–$5p5d\,^3D_1$, $5p^2\,^3P_0$–$5s5p\,^{1,3}P_1$, $5p^2\,^3P_0$–$5s5p\,^3D_1$, $5p^2\,^1S_0$–$5s5p\,^3P_1$, and $5p^2\,^1S_0$–$5s5p\,^3D_1$ transitions. It should be noted that only the two $5s^2\,^1S_0$–$5s5p\,^3P_1$ and $5s^2\,^1S_0$–$5s5p\,^1P_1$ transitions shown on the left top panel of Fig. 6 (curves "1" and "2") are the $5s$–$5p$ electric-dipole one-particle transitions. The other three transitions (curves "3", "4,' and "5") are forbidden as electric-dipole one-particle transitions. The values of the transition rates for these transitions are nonzero because of two-particle interactions between the $[5s^2+5p^2+5d^2]$ and $[5s5p+5p5d]$ configurations as well as because of the second-order contribution $Z^{(2)}$ as demonstrated in Table V (see details in Refs. [26,32]). As a result, the rates of these two-particle $5s^2\,^1S_0$–$5p5d\,^{1,3}P_1$ and $5s^2\,^1S_0$–$5d5f\,^1P_1$ transitions presented on the left top panel of Fig. 6 are smaller (by two to four orders of magnitude) than the rates of the one-particle $5s^2\,^1S_0$–$5s5p\,^{1,3}P_1$ transitions for smaller Z but become even larger for higher Z. Similar ratios between the allowed $5p^2$–$5p5d$ electric-dipole one-particle transitions and the forbidden $5p^2$–$5d5f$ electric-dipole two-particle transitions are demonstrated by the top right panel of Fig. 6.

In the two bottom panels of Fig. 6, we present a selected set of transition rates for the $5s5g$–$5p5g$ and $5p5f$–$5p5g$ transitions (8 among the 20 transitions between the states from

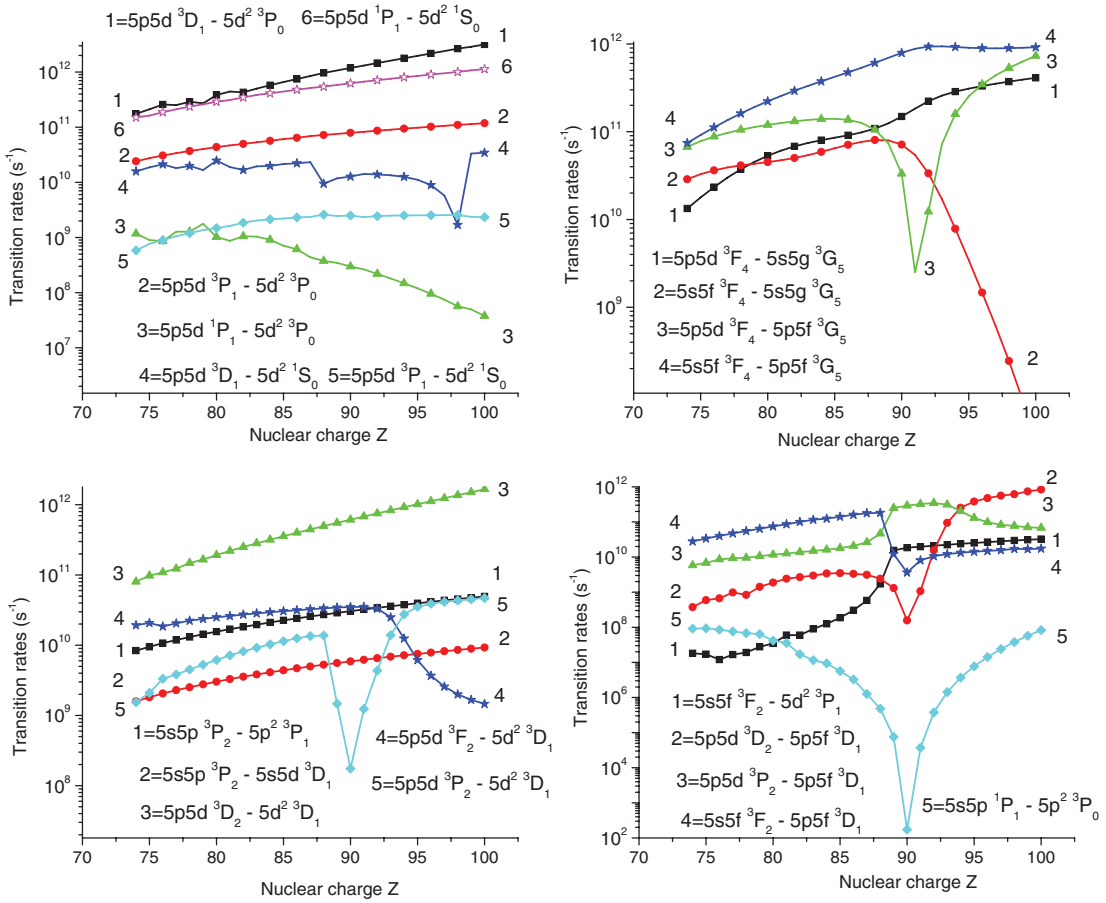

FIG. 7. (Color online) Transition rates for odd-even transitions in Sm-like ions as a function of Z.

the even-parity complex with $J = 5$ and odd-parity complexes with $J = 5$ and 6). The $5s5g$–$5p5g$ and $5p5f$–$5p5g$ transitions are illustrated by the $5s5g\ ^3G_5$–$5p5g\ ^3G_5$, $5s5g\ ^3G_5$–$5p5g\ ^{1,3}H_5$, $5p5f\ ^3G_5$–$5p5g\ ^3G_5$, and $5p5f\ ^3G_5$–$5p5g\ ^{1,3}H_5$ transitions shown on the bottom left panel of Fig. 6. On the bottom right panel of Fig. 6, the Z dependence of transition rates for the $5s5g\ ^3G_5$–$5p5g\ ^3H_6$ and $5p5f\ ^3G_5$–$5p5g\ ^3H_6$ transitions is highlighted.

In the four panels of Fig. 7, we present a selection of the electric-dipole one-electron $5s5p$–$5p^2$, $5s5p$–$5s5d$, $5p5d$–$5d^2$, $5p5d$–$5p5f$, and $5s5f$–$5p5f$ transitions, as well as electric-dipole two-electron $5p5d$–$5s5g$ and $5s5f$–$5d^2$ transitions. The smallest transition rates values are observed in Fig. 7 for singlet-triplet transitions: curves "3," "4," and 5" (top left panel) and curve "5" (bottom right panel), as well as for two-electron transitions: curve "1" (bottom right panel) and curve "1" (top right panel). In some cases this statement is not valid for high-Z ions (see, for example, curves "1" on the two right panels of Fig. 7).

We see from the graphs that transitions with smooth Z dependencies are rarer than transitions with sharp features but they still occur for all transition types: triplet-triplet, singlet-singlet, and singlet-triplet, and include transitions with both small J and larger J. However, we can make a general conclusion from those graphs, that the smooth Z dependencies occur more frequently for transitions with the largest rates among the transitions inside complexes.

Singularities in the transition-rate curves have three distinct origins: avoided level crossings, zeros in the dipole matrix elements, and zeros in transition energies. Avoided level crossings result in changes of the dominant level configuration at a particular value of Z and lead to abrupt changes in the transition-rate curves when the rates associated with the dominant configurations below and above the crossing point are significantly different. Zeros in transition matrix elements as functions of Z lead to cusplike minima in the transition-rate curves. Zeros in transition energies occur when levels of different parity cross.

Examples of each of these three singularity types can be found in Figs. 6 and 7. A dramatic example of the first type, i.e., that of an avoided level crossing, is seen in the bottom right panel of Fig. 7 around $Z = 87$–90, corresponding to a change in the dominant configuration for the $5s5f\ ^3F_2$ state, the $5p_{3/2}5d_{5/2}(2)$ instead of the $5s_{1/2}5f_{5/2}(2)$ configuration. Examples of the second type, i.e., zeros in matrix elements, are seen on the bottom right panel of Fig. 6 at $Z = 85$, the bottom left panel of Fig. 7 at $Z = 90$ for the $5p5d\ ^3P_2$–$5d^2\ ^3D_1$ transition, and the top right panel of Fig. 7 at $Z = 91$ for the $5p5d\ ^3F_4$–$5p5f\ ^3G_5$ transition. Finally, a singularity of the third type, corresponding to a very small (near zero) transition energy is seen at $Z = 90$ in the bottom right panel of Fig. 7 for the $5s5p\ ^1P_1 - 5p^2\ ^3P_0$ transition. In this case, the level inversion occurs at the interface between the upper even- and odd-parity groups at high Z. The upper $5p^2\ ^3P_0$ level

TABLE VIII. Energies (in cm^{-1}) and lifetimes τ (in ns) for Sm-like W^{12+}. Energies are given relative to the ground state. Energies and lifetimes of the odd- and even-parity states are calculated in first-order and second-order RMBPT (columns labeled RMBPT1 and RMBPT2, respectively) and the Hartree-Fock relativistic method implemented in COWAN code (column "COWAN").

LS coupl.	RMBPT1	RMBPT2 (Energies in cm^{-1})	COWAN	RMBPT1	RMBPT2 (Lifetimes in ns)	COWAN1	COWAN2 (Lifetimes in ns)	jj coupl.
$5s5p\,^3P_1$	243019	252360	242071	0.5236	0.6803	0.4200	0.4138	$5s_{1/2}5p_{1/2}(1)$
$5s5p\,^1P_1$	394436	392166	390296	0.0150	0.0223	0.0453	0.0382	$5s_{1/2}5p_{3/2}(1)$
$5p2\,^3P_0$	532126	534542	532140	0.0314	0.0488	0.0338	0.0337	$5p_{1/2}5p_{1/2}(0)$
$5p2\,^3P_1$	619166	628243	623802	0.0181	0.0271	0.0204	0.0200	$5p_{1/2}5p_{3/2}(1)$
$5p2\,^1D_2$	621224	634556	627570	0.0389	0.0558	0.0414	0.0370	$5p_{1/2}5p_{3/2}(2)$
$5p2\,^3P_2$	718323	735575	725900	0.0178	0.0252	0.0230	0.0206	$5p_{3/2}5p_{3/2}(2)$
$5s5d\,^3D_1$	753922	767330	755687	0.0082	0.0114	0.0115	0.0108	$5s_{1/2}5d_{3/2}(1)$
$5s5d\,^3D_2$	760078	773522	761945	0.0090	0.0124	0.0116	0.0110	$5s_{1/2}5d_{3/2}(2)$
$5p2\,^1S_0$	768138	774936	766355	0.0137	0.0186	0.0408	0.0156	$5p_{3/2}5p_{3/2}(0)$
$5s5d\,^3D_3$	771054	785580	773229	0.0120	0.0165	0.0283	0.0220	$5s_{1/2}5d_{5/2}(3)$
$5s5d\,^1D_2$	820724	820125	812408	0.0069	0.0095	0.0268	0.0092	$5s_{1/2}5d_{5/2}(2)$
$5p5d\,^3F_2$	997932	1022218	1009023	0.0608	0.0788	0.0564	0.0551	$5p_{1/2}5d_{3/2}(2)$
$5p5d\,^3D_1$	1047611	1057013	1050759	0.0059	0.0080	0.0054	0.0054	$5p_{1/2}5d_{3/2}(1)$
$5p5d\,^3F_3$	1035092	1057556	1044407	0.0276	0.0348	0.0260	0.0240	$5p_{1/2}5d_{5/2}(3)$
$5p5d\,^3P_2$	1042759	1058389	1048952	0.0115	0.0151	0.0123	0.0115	$5p_{1/2}5d_{5/2}(2)$
$5p5d\,^1D_2$	1121373	1143187	1131567	0.0080	0.0106	0.0075	0.0073	$5p_{3/2}5d_{3/2}(2)$
$5p5d\,^3F_4$	1115789	1147320	1129346	0.0775	0.1147	0.1274	0.0640	$5p_{3/2}5d_{5/2}(4)$
$5p5d\,^3D_3$	1131918	1151454	1140436	0.0069	0.0094	0.0067	0.0064	$5p_{3/2}5d_{3/2}(3)$
$5p5d\,^3P_0$	1136677	1153629	1144141	0.0070	0.0100	0.0065	0.0064	$5p_{3/2}5d_{3/2}(0)$
$5p5d\,^3P_1$	1139489	1155894	1146453	0.0065	0.0091	0.0060	0.0060	$5p_{3/2}5d_{3/2}(1)$
$5p5d\,^3P_2$	1148161	1165777	1155195	0.0076	0.0104	0.0079	0.0076	$5p_{3/2}5d_{5/2}(2)$
$5p5d\,^3D_3$	1162428	1182089	1170144	0.0077	0.0101	0.0081	0.0074	$5p_{3/2}5d_{5/2}(3)$
$5p5d\,^1P_1$	1197346	1206025	1195023	0.0074	0.0099	0.0083	0.0075	$5p_{3/2}5d_{5/2}(1)$

becomes the lower $5p^2\,^3P_0$ level, while the lower $5s5p\,^1P_1$ level becomes the upper level at $Z = 90$.

VI. LIFETIMES IN Sm-LIKE W^{12+} ION

Energies and lifetimes for low-lying levels in Sm-like W^{12+} ion are given in Table VIII. In this table, we list lifetimes calculated in the first-order and second-order RMBPT (columns labeled "RMBPT1" and "RMBPT2", respectively). Additionally, we included and lifetimes evaluated by the Hartree-Fock relativistic method (COWAN code). In column "COWAN1", we present the lifetimes obtained by including the $5l_15l_2 - 5l_35l_4$ transitions. The lifetimes in the column "COWAN2" are obtained by including additional transitions involving the core-excited states such as the $4f^{13}5s^25p - 4f^{14}5s5p$, $4f^{13}5s5p^2 - 4f^{14}5p^2$, $4f^{13}5s5p^2 - 4f^{14}5s5d$, and $4f^{13}5s5p5d - 4f^{14}5p5d$ transitions. The number of decay channels is substantially increased; five channels instead of one channel for the lifetime of the $4f^{14}5s5p\,^3P_1$ level and 23 instead of 4 for the lifetime of the $4f^{14}5p^2\,^3P_1$ level. This increase in the numbers of channels does not necessary lead to a substantial change of the lifetimes values. We can see from a comparison of the lifetimes given in columns "COWAN1" and "COWAN2" of Table VIII that the difference is about 1-10% except for the lifetimes of three levels ($5p^2\,^1S_0$, $5s5d\,^1D_2$, and $5p5d\,^3F_4$), for which the difference is about a factor of 2-3. Those changes in the lifetimes of the $5p^2\,^1S_0$ and $5s5d\,^1D_2$ levels produce excellent agreement with the lifetimes given in column "RMBPT2" of Table VIII. Comparison of the lifetimes given in columns "RMBPT1" and "RMBPT2" gives us an estimate of the correlation contribution, which is found to be about 20-30%.

VII. UNCERTAINTY ESTIMATES AND CONCLUSION

The comparison of the RMBPT1 and RMBPT2 energies and transition rates presented in Tables IV, VII, and VIII gives us a first, rough estimate of the uncertainties of our results through the second-order correlation correction. The differences in the RMBPT1 and RMBPT2 values are about 1%–3% for energies, about 20%–30% for the largest values of transitions rates A_r, and a factor of 2–3 for the smallest values of A_r. The comparison of the lifetimes evaluated by the RMBPT1 and RMBPT2 codes gives us an estimation of the correlation contribution, which is about 20%–30%. The third-order corrections for the energies and transition rates were evaluated for monovalent atomic systems (see, for example, Refs. [46–48]). The differences between the RMBPT3 and RMBPT2 energies were about 2%–3% for Ba II, Sr II, and Hg II ions. In addition, we evaluated the energies and transition rates in Sm-like Re^{13+}, Os^{14+}, Ir^{15+}, Pt^{16+}, Au^{17+}, Ra^{26+}, and U^{30+} ions using the COWAN code. These results are between our RMBPT1 and RMBPT2 values (see Tables IV and VIII).

To check the accuracy of our RMBPT results for the radiative lifetimes of levels in the Sm-like W^{12+} ion, we evaluated the lifetimes with and without core-excited states using the Hartree-Fock relativistic method (COWAN code). The

differences were about 1%–10% except for the lifetimes of the three levels $5p^2\,{}^1S_0$, $5s5d\,{}^1D_2$, and $5p5d\,{}^3F_4$, for which the difference was about a factor of 2–3. This means that the including of core-excited states in the evaluation of lifetimes in the COWAN code leads to changes of the correlation contribution about equal to the RMBPT correlation contributions.

We have presented a systematic second-order relativistic MBPT study of excitation energies, oscillator strengths, transition probabilities, and lifetimes in Sm-like ions with nuclear charge Z ranging from 74 to 100. Our reduced matrix elements included correlation corrections from Coulomb and Breit interactions. We determined energies of the $5s_{1/2}5p_j(J)$, $5s_{1/2}5d_j(J)$, $5s_{1/2}5f_j(J)$, $5s_{1/2}5g_j(J)$, $5p_j5d_{j'}(J)$, $5p_j5d_{j'}(J)$, $5p_j5f_{j'}(J)$, $5p_j5g_{j'}(J)$, and $5d_j5d_{j'}(J)$ excited states. Wavelengths, line strengths, oscillator strengths, and transition rates were evaluated for the 567 dipole matrix elements for transitions between the 35 even-parity states and the 32 odd-parity states in Sm-like ions. The resulting transition energies and transition probabilities, and lifetimes for Sm-like W^{12+} were compared with results obtained by the relativistic Hartree-Fock approximation (COWAN code) to estimate the contributions of the $4f$-core-excited states. Trends of excitation energies and oscillator strengths as a function of nuclear charge Z were shown graphically for selected states and transitions. Our RMBPT results presented in this paper are *ab initio* calculations of energies, and transition rates in Sm-like ions. This work provides a starting point for further development of theoretical methods for such highly correlated and relativistic systems.

ACKNOWLEDGMENTS

This research was sponsored by DOE under the OFES Grant No. DE-FG02-08ER54951 and in part under the NNSA CA DE-FC52-06NA27588. Work at the Lawrence Livermore National Laboratory was performed under auspices of the DOE under Contract No. DE-AC52-07NA-27344.

[1] A. Kramida, Yu. Ralchenko, J. Reader, and the NIST ASD Team, NIST Atomic Spectra Database (version 5.0), http://physics.nist.gov/asd, National Institute of Standards and Technology, Gaithersburg, MD.

[2] E. Biémont, G. Kohnen, and P. Quinet, Astron. Astrophys. **393**, 717 (2002).

[3] J. Clementson, P. Beiersdorfer, G. Brown, M. Gu, H. Lundberg, Y. Podpaly, and E. Träbert, Can. J. Phys. **89**, 571 (2011).

[4] P. Beiersdorfer, J. K. Lepson, M. B. Schneider, and M. P. Bode, Phys. Rev. A **86**, 012509 (2012).

[5] C. Suzuki, C. S. Harte, D. Kilbane, T. Kato, H. A. Sakaue, I. Murakami, D. Kato, K. Sato, N. Tamura, S. Sudo *et al.*, J. Phys. B **44**, 175004 (2011).

[6] C. Suzuki, C. S. Harte, D. Kilbane, T. Kato, H. A. Sakaue, I. Murakami, D. Kato, K. Sato, N. Tamura, S. Sudo *et al.*, AIP Conf. Proc. No. 1438 (AIP, Melville, NY, 2012), p. 197.

[7] J. Clementson, P. Beiersdorfer, E. W. Magee, H. S. McLean, and R. D. Wood, J. Phys. B **43**, 144009 (2010).

[8] J. Clementson, P. Beiersdorfer, and M. F. Gu, Phys. Rev. A **81**, 012505 (2010).

[9] J. Clementson, P. Beiersdorfer, G. V. Brown, and M. F. Gu, Phys. Scr. **81**, 015301 (2010).

[10] P. Beiersdorfer, G. V. Brown, J. Clementson, J. Dunn, K. Morris, E. Wang, R. L. Kelley, C. A. Kilbourne, F. S. Porter, M. Bitter *et al.*, Rev. Sci. Instrum. **81**, 10E323 (2010).

[11] C. S. Harte, C. Suzuki, T. Kato, H. A. Sakaue, D. Kato, K. Sato, N. Tamura, S. Sudo, R. D'Arcy, and E. Sokell, J. Phys. B **43**, 205004 (2010).

[12] J. Clementson and P. Beiersdorfer, Phys. Rev. A **81**, 052509 (2010).

[13] P. Beiersdorfer, J. Clementson, J. Dunn, M. F. Gu, K. Morris, Y. Podpaly, E. Wang, M. Bitter, R. Feder, K. Hill *et al.*, J. Phys. B **43**, 144008 (2010).

[14] J. Clementson, P. Beiersdorfer, A. L. Roquemore, C. H. Skinner, D. K. Manseld, K. Hartzfeld, and J. K. Lepson, Rev. Sci. Instrum. **81**, 10E326 (2010).

[15] M. Reinke, P. Beiersdorfer, N. T. Howard, E. W. Magee, Y. Podpaly, J. E. Rice, and J. L. Terry, Rev. Sci. Instrum. **81**, 10D736 (2010).

[16] J. Yanagibayashi, T. Nakano, A. Iwamae, H. Kubo, M. Hasuo, and K. Itami, J. Phys. B **43**, 144013 (2010).

[17] C. H. Skinner, Can. J. Phys. **86**, 285 (2008).

[18] P. Beiersdorfer, G. V. Brown, A. T. Graf, M. Bitter, K. W. Hill, R. L. Kelley, C. A. Kilbourne, M. A. Leutenegger, and F. S. Porter, Rev. Sci. Instrum. **83**, 10E111 (2012).

[19] U. I. Safronova, A. S. Safronova, and P. Beiersdorfer, J. Phys. B **45**, 085001 (2012).

[20] U. I. Safronova and A. S. Safronova, Phys. Rev. A **85**, 032507 (2012).

[21] U. I. Safronova and A. S. Safronova, Phys. Rev. A **84**, 012511 (2011).

[22] U. I. Safronova and A. S. Safronova, J. Phys. B **45**, 185002 (2012).

[23] S. Enzonga Yoca, P. Quinet, and É. Biémont, J. Phys. B **45**, 035001 (2012).

[24] M. S. Safronova, W. R. Johnson, and U. I. Safronova, Phys. Rev. A **53**, 4036 (1996).

[25] M. S. Safronova, W. R. Johnson, and U. I. Safronova, J. Phys. B **30**, 2375 (1997).

[26] U. I. Safronova, W. R. Johnson, M. S. Safronova, and A. Derevianko, Phys. Scr. **59**, 286 (1999).

[27] U. I. Safronova, A. Derevianko, M. S. Safronova, and W. R. Johnson, J. Phys. B **32**, 3527 (1999).

[28] U. I. Safronova, W. R. Johnson, and H. G. Berry, Phys. Rev. A **61**, 052503 (2000).

[29] U. I. Safronova, Mol. Phys. **98**, 1213 (2000).

[30] U. I. Safronova, W. R. Johnson, D. Kato, and S. Ohtani, Phys. Rev. A **63**, 032518 (2001).

[31] S. A. Blundell, W. R. Johnson, M. S. Safronova, and U. I. Safronova, Phys. Rev. A **77**, 032507 (2008).

[32] U. I. Safronova and M. S. Safronova, J. Phys. B **43**, 074025 (2010).

[33] U. I. Safronova, W. R. Johnson, M. S. Safronova, and J. R. Albritton, Phys. Rev. A **66**, 022507 (2002).
[34] U. I. Safronova and A. S. Safronova, J. Phys. B **43**, 074026 (2010).
[35] W. R. Johnson, S. A. Blundell, and J. Sapirstein, Phys. Rev. A **37**, 2764 (1988).
[36] M. H. Chen, K. T. Cheng, and W. R. Johnson, Phys. Rev. A **47**, 3692 (1993).
[37] L. W. Fullerton and G. A. Rinker, Jr., Phys. Rev. A **13**, 1283 (1976).
[38] P. J. Mohr, Ann. Phys. (NY) **88**, 26 (1974).
[39] P. J. Mohr, Ann. Phys. (NY) **88**, 52 (1974).
[40] P. J. Mohr, Phys. Rev. Lett. **34**, 1050 (1975).
[41] U. I. Safronova, W. R. Johnson, A. Shlyaptseva, and S. Hamasha, Phys. Rev. A **67**, 052507 (2003).
[42] R. D. Cowan, *The Theory of Atomic Structure and Spectra* (University of California Press, Berkeley, 1981).
[43] B. C. Fawcett, N. J. Peacock, and R. D. Cowan, J. Phys. B **1**, 295 (1968).
[44] M. S. Safronova, M. G. Kozlov, W. R. Johnson, and Dansha Jiang, Phys. Rev. A **80**, 012516 (2009).
[45] L. D. Landau and E. M. Lifshitz, *Quantum Mechanics-Non-Relativistic Theory* (Pergamon Press, London, 1963), p. 281.
[46] U. I. Safronova, Phys. Rev. A **81**, 052506 (2010).
[47] U. I. Safronova, Phys. Rev. A **82**, 022504 (2010).
[48] U. I. Safronova and W. R. Johnson, Phys. Rev. A **69**, 052511 (2004).